



ARTICLE

Stability and Bifurcation of a Prey-Predator System with Additional Food and Two Discrete Delays

Ankit Kumar and Balram Dubey*

Department of Mathematics, BITS Pilani, Pilani Campus, Pilani, 333031, India

*Corresponding Author: Balram Dubey. Email: bdubey@pilani.bits-pilani.ac.in

Received: 29 July 2020 Accepted: 22 October 2020

ABSTRACT

In this paper, the impact of additional food and two discrete delays on the dynamics of a prey-predator model is investigated. The interaction between prey and predator is considered as Holling Type-II functional response. The additional food is provided to the predator to reduce its dependency on the prey. One delay is the gestation delay in predator while the other delay is the delay in supplying the additional food to predators. The positivity, boundedness and persistence of the solutions of the system are studied to show the system as biologically well-behaved. The existence of steady states, their local and global asymptotic behavior for the non-delayed system are investigated. It is shown that (i) predator's dependency factor on additional food induces a periodic solution in the system, and (ii) the two delays considered in the system are capable to change the status of the stability behavior of the system. The existence of periodic solutions via Hopf-bifurcation is shown with respect to both the delays. Our analysis shows that both delay parameters play an important role in governing the dynamics of the system. The direction and stability of Hopf-bifurcation are also investigated through the normal form theory and the center manifold theorem. Numerical experiments are also conducted to validate the theoretical results.

KEYWORDS

Additional food; Gestation delay; Hopf-bifurcation; Prey-predator

1 Introduction

Living organisms on the surface of the earth adopt only the way that boosts their survival possibilities so that they can pass their genes to the next generation. There are several fundamental instincts in ecological communities and, predation is one of them that constitutes the building blocks for multispecies food webs. Initially, Lotka [1] and Volterra [2] studied the model for prey-predator interaction and observed the uniform fluctuations in the time series of the system. On later the fluctuations were removed from the system by taking logistic growth of prey population [3,4]. Many researchers have widely studied prey-predator interactions for the last century [5–12]. They have considered several essential concepts over time that play a vital role in the dynamics of the system like functional response, time delay, harvesting and conservation policies of species, stage structure, fear induced by predators, etc. The idea of functional response was proposed by Holling [5]. It is defined as the consumption rate of prey by predators. Holling



considered it nonlinear function of prey species that saturates at a level. Further, it was considered a function of prey and predator both by several authors [6,10,13,14].

In last few decades, many authors have studied the qualitative dynamics of prey-predator systems in the presence of additional food resources for predators [15–20]. Additional food is an important component for predators like coccinellid which shapes the life history of many predator species [17]. Ghosh et al. [20] investigated the impact of additional food for predator on the dynamics of prey-predator model with prey refuge and they observed that predator extinction possibility in high prey refuge may be removed by providing additional food to predators. Again, to study the role of additional food in an eco-epidemiological system, a model was proposed and studied by Sahoo [21]. The author found that the system becomes disease free in presence of suitable additional food provided to predator. Recently, a prey-predator model with harvesting and additional food is analyzed by Rani et al. [22] and they have shown some local and global bifurcation with respect to different parameters. To incorporate the additional food into the model, they modified the Holling type II functional response.

Delayed models exhibit much more realistic dynamics than non delayed models [4,23]. In prey-predator system, the impact of consumed prey individuals into predator population does not appear immediately after the predation, there is some time lag that is gestation delay [24]. We incorporate the effect of time delay into the model with delay differential equations. A delay differential equation demonstrates much more complex character than ordinary differential equation. On the other hand predators do not consume the additional food as soon as it is provided. They take some time to consume and digest the food. Delayed models are widely studied by researchers [10,14,25–33]. A delayed prey and predator density dependent system is investigated by Li et al. [10]. The authors analyzed stability, Hopf-bifurcation and its qualitative properties by using Poincare normal form and the formulae given in Hassard et al. [34]. Sahoo et al. [35] examined prey-predator model with effects of supplying additional food to predators in a gestation delay induced prey-predator system and habitat complexity. They have pointed out that Hopf-bifurcation occurs in the system when delay crosses a threshold value that strongly depends on quality and quantity of supplied additional food. The effect of additional food along with fear induced by predators and gestation delay is discussed by Mondal et al. [36]. There are several studies carried out with multiple delays [37–40]. Li et al. [37] have done stability and Hopf-bifurcation analysis of a prey-predator model with two maturation delays. Gakkhar et al. [30] explored the complex dynamics of a prey-predator system with multiple delays. They established the presence of periodic orbits via Hopf-bifurcation with respect to both delays. Recently, Kundu et al. [40] have discussed about the dynamics of two prey and one predator system with cooperation among preys against predators incorporating three discrete delays. The authors have found that all delays are capable to destabilize the system.

To the best of our knowledge, an ecological model including (i) Effect of additional food supplies to predators, (ii) Dependency factor of supplied additional food, (iii) Holling Type II functional response, (iv) Gestation delay in predator have not been considered. Inspired by this, we establish three dimensional non delayed and delayed models in Section 2. We analyze the dynamics of non delayed model and validate it via some numerical simulations in Section 3. In Section 4, we analyze the dynamics of delayed model through Hopf-bifurcation. Direction and stability of Hopf-bifurcation are carried out in Section 5. Section 6 is devoted to the numerical simulations for delayed model. Conclusions and significance of this work are discussed briefly in Section 7.

2 Proposed Mathematical Model

We consider a habitat where two biological populations, prey population and predator population are surviving and interacting with each other. It is assumed that prey population grows logistically and the interaction between prey and predator follows Holling Type II functional response. We assume that the density of the additional food supplied to the predators is directly proportional to the density of predators present in the habitat. Keeping these in view, the dynamics of the system can be governed by the following system of differential equations:

$$\begin{cases} \frac{dx}{dt} = rx \left(1 - \frac{x}{K}\right) - \frac{\alpha(1 - A_0)xy}{1 + ax}, \\ \frac{dA}{dt} = \lambda A_0 y - \beta A - \phi Ay, \\ \frac{dy}{dt} = \frac{c_1 \alpha(1 - A_0)xy}{1 + ax} + c_2 \phi Ay - dy - ey^2, \\ x(0) \geq 0, \quad A(0) \geq 0, \quad y(0) \geq 0. \end{cases} \tag{1}$$

In the above model $x(t)$, $y(t)$ are number of prey and predator individuals at time t and A is quantity of additional food provided to predators. A_0 is dependency factor of predators on provided additional food resources. If $A_0 = 1$, then predators depend completely on additional food and prey population grows logistically. If $A_0 = 0$, then predators depend only on the prey population and in such a case additional food is not required. λ is maximum supply rate of additional food resources.

In real situations, each organism needs an amount of time to reproduce their progeny. Due to this fact the increment in predators does not appear immediately after consuming prey. It is assumed that a predator individual takes τ_1 time for gestation. Therefore, it seems reasonable to incorporate a gestation delay in the system. Thus, the delay τ_1 is considered in the numeric response only. Again it is assumed that the additional food is provided to predators with another delay τ_2 . The generalized model involving these two discrete delays takes the following form

$$\begin{cases} \frac{dx}{dt} = rx \left(1 - \frac{x}{K}\right) - \frac{\alpha(1 - A_0)xy}{1 + ax}, \\ \frac{dA}{dt} = \lambda A_0 y - \beta A - \phi Ay, \\ \frac{dy}{dt} = \frac{c_1 \alpha(1 - A_0)x(t - \tau_1)y(t - \tau_1)}{1 + ax(t - \tau_1)} + c_2 \phi A(t - \tau_2)y(t - \tau_2) - dy - ey^2, \end{cases} \tag{2}$$

subject to the non negative conditions $x(s) = \phi_1(s) \geq 0$, $A(s) = \phi_2(s) \geq 0$, $y(s) = \phi_3(s) \geq 0$, $s \in [-\tau, 0]$, where $\tau = \max\{\tau_1, \tau_2\}$ and $\phi_i(s) \in C([-\tau, 0] \rightarrow R_+)$, $(i = 1, 2, 3)$.

The biological meaning of all parameters and variables in above models is provided in [Tab. 1](#).

Table 1: Variables and parameters used in Models (1) & (2)

Variables/ parameters	Biological meaning	Unit
x	Density of prey population	Number per unit area (tons)
A	Quantity of additional food	Number per unit area (tons)
y	Density of predator population	Number per unit area (tons)
r	Intrinsic growth rate of prey	Per day
K	Carrying capacity of the prey population	Number per unit area (tons)
α	Attack rate of predator on prey	Per day
A_0	Dependency factor of predators on provided additional food	Constant & $0 \leq A_0 \leq 1$
a	Handling time	Days
λ	Maximum supply rate of additional food	Per day
β	Natural depletion rate of additional food	Per day
ϕ	Consumption rate of additional food by predators	Per day
c_1	Conversion efficiency of y on x	Constant & $0 \leq c_1 \leq 1$
c_2	Conversion efficiency of y on A	Constant & $0 \leq c_2 \leq 1$
d	Mortality rate of predators	Per day
e	Intra-specific interference among predators	Per day
τ_1	Gestation delay of predators	Days
τ_2	Delay in supply of the additional food	Days

3 Dynamics of Non-delayed Model

First of all, we examine the boundedness and persistence of the system (1).

3.1 Boundedness and Persistence of the Solution

Theorem 3.1. The set

$$\Omega = \left\{ (x, A, y) : 0 \leq x \leq K, 0 \leq c_1x + c_2A + y \leq \frac{1}{\delta} \left[2c_1rK + \frac{c_2^2\lambda^2A_0^2}{4e} \right] \right\}$$

is a positive invariant set for all the solutions of model (1), initiating in the interior of the positive octant, where $\delta = \min\{r, \beta, d\}$.

Proof The model system (1) can be written in the matrix form

$$\dot{X} = G(X),$$

where $X = (x_1, x_2, x_3)^T = (x, A, y)^T \in R^3$, and $G(X)$ is given by

$$G(X) = \begin{bmatrix} G_1(X) \\ G_2(X) \\ G_3(X) \end{bmatrix} = \begin{bmatrix} rx \left(1 - \frac{x}{K}\right) - \frac{\alpha(1 - A_0)xy}{1 + ax} \\ \lambda A_0y - \beta A - \phi Ay \\ \frac{c_1\alpha(1 - A_0)xy}{1 + ax} + c_2\phi Ay - dy - ey^2 \end{bmatrix}$$

Since $G: R^3 \rightarrow R^3_+$ is locally Lipschitz-continuous in Ω and $X(0) = X_0 \in R^3_+$, the fundamental theorem of ordinary differential equation guarantees the local existence and uniqueness of the solution. Since $[G_i(X)]_{x_i(t)=0, X \in R^3_+} \geq 0$, it follows that $X(t) \geq 0$ for all $t \geq 0$. In fact, from the first equation of model (1), it can easily be seen that $\dot{x}|_{x=0} \geq 0, \dot{y}|_{y=0} \geq 0$ and hence $x(t) \geq 0, y(t) \geq 0$ for all $t \geq 0$. Secondly, $\dot{A}|_{A=0} = \lambda A_0 y \geq 0$ for all $t \geq 0$ (as $y(t) \geq 0$ for all $t \geq 0$.) and hence $A(t) \geq 0$ for all $t \geq 0$.

From the first equation of model (1), we can write

$$\frac{dx}{dt} \leq rx \left(1 - \frac{x}{K}\right),$$

which yields

$$\limsup_{t \rightarrow \infty} x(t) \leq K.$$

Now, suppose

$$W(t) = c_1x(t) + c_2A(t) + y(t),$$

then we have

$$\begin{aligned} \frac{dW(t)}{dt} &= c_1 \frac{dx}{dt} + c_2 \frac{dA}{dt} + \frac{dy}{dt} \leq 2c_1rK - c_1rx - dy + c_2\lambda A_0y - c_2\beta A - ey^2 \\ &\leq 2c_1rK + \frac{c_2^2\lambda^2A_0^2}{4e} - \left(\sqrt{e}y - \frac{c_2\lambda A_0}{2\sqrt{e}}\right)^2 - \delta W, \end{aligned}$$

where $\delta = \min\{r, \beta, d\}$.

Hence, it follows that

$$\limsup_{t \rightarrow \infty} W(t) \leq \frac{1}{\delta} \left(2c_1rK + \frac{c_2^2\lambda^2A_0^2}{4e}\right) =: y_s.$$

We also note that if $x(t) \geq K$ and $W(t) \geq \frac{1}{\delta} \left(2c_1rK + \frac{c_2^2\lambda^2A_0^2}{4e}\right)$, then $\frac{dx(t)}{dt} \leq 0, \frac{dW(t)}{dt} \leq 0$.

This shows that all solutions of system (1) are bounded and remains in Ω for all $t > 0$ if $(x(0), A(0), y(0)) \in \Omega$.

Theorem 3.2. Let the following inequalities are satisfied:

$$r > \alpha(1 - A_0)y_s, \quad \frac{c_1\alpha(1 - A_0)x_a}{1 + ax_a} > d.$$

Then model system (1) is uniformly persistence, where, x_a is defined in the proof.

Proof: System (1) is said to be permanence or uniform persistence if there are positive constants M_1 and M_2 such that each positive solution $X(t) = (x(t), A(t), y(t))$ of the system with positive initial conditions satisfies

$$M_1 \leq \liminf_{t \rightarrow \infty} X(t) \leq \limsup_{t \rightarrow \infty} X(t) \leq M_2.$$

Keeping the above in view, if we define

$$M_2 = \max \left\{ K, \frac{y_s}{c_2}, y_s \right\},$$

then from Theorem 3.1, it follows that

$$\limsup_{t \rightarrow \infty} X(t) \leq M_2.$$

This also shows that for any sufficiently small $\varepsilon > 0$, there exists a $T > 0$ such that for all $t \geq T$, the following holds:

$$x(t) < K + \varepsilon, \quad A(t) < \frac{y_s}{c_2} + \varepsilon, \quad y(t) < y_s + \varepsilon.$$

Now from the first equation of model system (1), for all $t \geq T$, we can write

$$\begin{aligned} \frac{dx}{dt} &\geq rx \left(1 - \frac{x}{K} \right) - \alpha(1 - A_0)(y_s + \varepsilon)x \\ &= [r - \alpha(1 - A_0)(y_s + \varepsilon)]x - \frac{rx^2}{K}. \end{aligned}$$

Hence, it follows that

$$\liminf_{t \rightarrow \infty} x(t) \geq \frac{K}{r} [r - \alpha(1 - A_0)(y_s + \varepsilon)],$$

which is true for every $\varepsilon > 0$, thus

$$\liminf_{t \rightarrow \infty} x(t) \geq \frac{K}{r} [r - \alpha(1 - A_0)y_s] =: x_a,$$

where $r > \alpha(1 - A_0)y_s$.

Now from the third equation of model system (1), we obtain

$$\frac{dy}{dt} \geq \frac{c_1 \alpha (1 - A_0) (x_a + \varepsilon) y}{1 + a(x_a + \varepsilon)} - dy - ey^2,$$

which implies

$$\liminf_{t \rightarrow \infty} y(t) \geq \frac{1}{e} \left[\frac{c_1 \alpha (1 - A_0) (x_a + \varepsilon)}{1 + a(x_a + \varepsilon)} - d \right],$$

which is true for every $\varepsilon > 0$, thus

$$\liminf_{t \rightarrow \infty} y(t) \geq \frac{1}{e} \left[\frac{c_1 \alpha (1 - A_0) x_a}{1 + ax_a} - d \right] =: y_a,$$

for persistence, we must have $\frac{c_1 \alpha (1 - A_0) x_a}{1 + ax_a} > d$.

Second equation of model system (1) yields

$$\frac{dA}{dt} \geq \lambda A_0(y_a + \varepsilon) - \beta A - \phi(y_s + \varepsilon)A.$$

Hence

$$\liminf_{t \rightarrow \infty} A(t) \geq \frac{\lambda A_0 y_a}{\beta + \phi y_s} =: A_a.$$

Taking $M_1 = \min\{x_a, A_a, y_a\}$, the theorem follows.

Remark. Theorem 3.2 shows that threshold values for the persistence of the system are dependent on the parameter A_0 .

3.2 Equilibrium Points and Their Stability Behavior

System (1) has four equilibrium points, trivial equilibrium $E_0(0,0,0)$, axial equilibrium $E_1(K,0,0)$, prey free equilibrium $E_2(0, \tilde{A}, \tilde{y})$ and interior equilibrium $E^*(x^*, A^*, y^*)$. E_0 and E_1 always exist.

- **Existence of $E_2(0, \tilde{A}, \tilde{y})$:** The prey free equilibrium E_2 is positive solution of the following system:

$$\begin{aligned} \lambda A_0 y - \beta A - \phi A y &= 0, \\ c_2 \phi A - d - e y &= 0. \end{aligned} \tag{3}$$

From the second equation of above system, we have

$$A = \frac{d + e y}{c_2 \phi}.$$

Putting the value of A in the first equation of system (3), we get

$$\phi e y^2 + (\phi d + \beta e - c_2 \phi \lambda A_0) y + \beta d = 0. \tag{4}$$

Above equation has two positive roots if

$$c_2 \phi \lambda A_0 > \phi d + \beta e, \quad (c_2 \phi \lambda A_0 - \phi d - \beta e)^2 > 4 \phi d \beta e. \tag{5}$$

System (1) has two prey free equilibrium under conditions given in (5): $\tilde{E}_2(0, \tilde{A}, \tilde{y})$ and $\hat{E}_2(0, \hat{A}, \hat{y})$. Again, If $c_2 \phi \lambda A_0 < \phi d + \beta e$, then Eq. (4) does not have any positive root. Therefore, E_2 does not exist in this case.

- **Existence of interior equilibrium $E^*(x^*, A^*, y^*)$:** It may be seen that x^*, A^* and y^* are the positive solution of the following system of algebraic equations:

$$\begin{aligned} r \left(1 - \frac{x}{K} \right) - \frac{\alpha(1 - A_0)y}{1 + ax} &= 0, \\ \lambda A_0 y - \beta A - \phi A y &= 0, \\ \frac{c_1 \alpha(1 - A_0)x}{1 + ax} + c_2 \phi A - d - e y &= 0. \end{aligned} \tag{6}$$

From the second equation of system (6), we have

$$A = \frac{\lambda A_0 y}{\beta + \phi y}.$$

Putting this into the first and third equation of system (6), we obtain the following system:

$$y = \frac{r}{\alpha(1-A_0)} \left(1 - \frac{x}{K}\right) (1+ax), \quad (7)$$

$$\frac{c_1 \alpha (1-A_0) x}{1+ax} + \frac{c_2 \phi \lambda A_0 y}{\beta + \phi y} - d - ey = 0 \quad (8)$$

We note the following points from Eq. (7):

1. When $y=0$, then $x = -\frac{1}{a} < 0$ or $x = K > 0$.
2. When $x=0$ then $y = \frac{r}{\alpha(1-A_0)} > 0$.
- 3.

$$\frac{dy}{dx} = \frac{r}{\alpha(1-A_0)} \left[a - \frac{1}{K} - \frac{2ax}{K} \right].$$

It also can be noted that $\frac{dy}{dx} > 0$ if $-\frac{1}{a} < x < \frac{1}{2} \left(K - \frac{1}{a} \right)$ and $\frac{dy}{dx} < 0$ if $x > \frac{1}{2} \left(K - \frac{1}{a} \right)$.

4. $y_{max} = \frac{1}{4} \left(1 + \frac{1}{ak} \right) (1+ak)$ at $x = \frac{1}{2} \left(K - \frac{1}{a} \right)$.

Similarly, from Eq. (8), we note the following:

1. When $y=0$, then $x = \frac{d}{c_1 \alpha (1-A_0) - ad}$.
- 2.

$$\frac{dy}{dx} = \frac{\frac{c_1 \alpha (1-A_0)}{(1+ax)^2}}{e - \frac{\beta c_2 \phi \lambda A_0}{(\beta + \phi y)^2}}.$$

It can be noted that $\frac{dy}{dx} > 0$ if

$$e(\beta + \phi y_a)^2 > \beta c_2 \phi \lambda A_0. \quad (9)$$

From above analysis we can conclude that system (6) has a unique positive solution (x^*, A^*, y^*) if, in addition to condition (9), the following holds:

$$0 < \frac{d}{c_1\alpha(1 - A_0) - ad} < K. \tag{10}$$

Hence, we can state the following theorem.

Theorem 3.3. The system (1) has a unique positive equilibrium $E^*(x^*, A^*, y^*)$ if (9) and (10) hold.

Remark. The number of positive equilibrium for the system (1) depends on values of parameters, which we have chosen. Several possibilities are depicted in Fig. 1.

The local behavior of a system in the vicinity of any existing equilibrium is very close to the behavior of its Jacobian system. So, we compute the Jacobian matrix to see the local behavior of the system around its equilibrium and we observe that

- The trivial equilibrium $E_0(0, 0, 0)$ is always a saddle point having stable manifold along the A and y -axes and unstable manifold along the x -axis.
- The axial equilibrium $E_1(K, 0, 0)$ is locally asymptotically stable if $\frac{c_1\alpha(1 - A_0)K}{1 + aK} < d$. If $\frac{c_1\alpha(1 - A_0)K}{1 + aK} > d$, then E_1 is a saddle point having stable manifold along the x and A -axes and unstable manifold along the y -axis.
- The Jacobian matrix evaluated at prey free equilibrium $E_2(0, \tilde{A}, \tilde{y})$ is given by

$$J|_{E_2} = \begin{bmatrix} r - \alpha(1 - A_0)\tilde{y} & 0 & 0 \\ 0 & -\frac{\lambda A_0 \tilde{y}}{\tilde{A}} & \lambda A_0 - \phi \tilde{A} \\ c_1\alpha(1 - A_0)\tilde{y} & c_2\phi \tilde{y} & -e\tilde{y} \end{bmatrix}$$

Characteristic equation is given by

$$(\zeta - (r - \alpha(1 - A_0))) \left[\zeta^2 + (\lambda A_0 \tilde{y} + e\tilde{y})\zeta + (e\lambda A_0 \tilde{y}^2 - c_2\phi \tilde{y}(\lambda A_0 - \phi \tilde{A})) \right] = 0. \tag{11}$$

The roots of Eq. (11) have negative real part if

$$r < \alpha(1 - A_0)\tilde{y}, \quad \lambda A_0 < \phi \tilde{A}. \tag{12}$$

Hence $\tilde{E}_2(0, \tilde{A}, \tilde{y})$ is asymptotically stable under condition (12).

Eq. (11) have at least one positive and one negative root if

$$e\lambda A_0 \tilde{y} < c_2\phi(\lambda A_0 - \phi \tilde{A}) \tag{13}$$

Therefore, $\tilde{E}_2(0, \tilde{A}, \tilde{y})$ is a saddle point under condition (13).

Remark. By replacing \tilde{A} by \hat{A} and \tilde{y} by \hat{y} , similar analysis holds good for the stability behavior of $\hat{E}_2(0, \hat{A}, \hat{y})$.

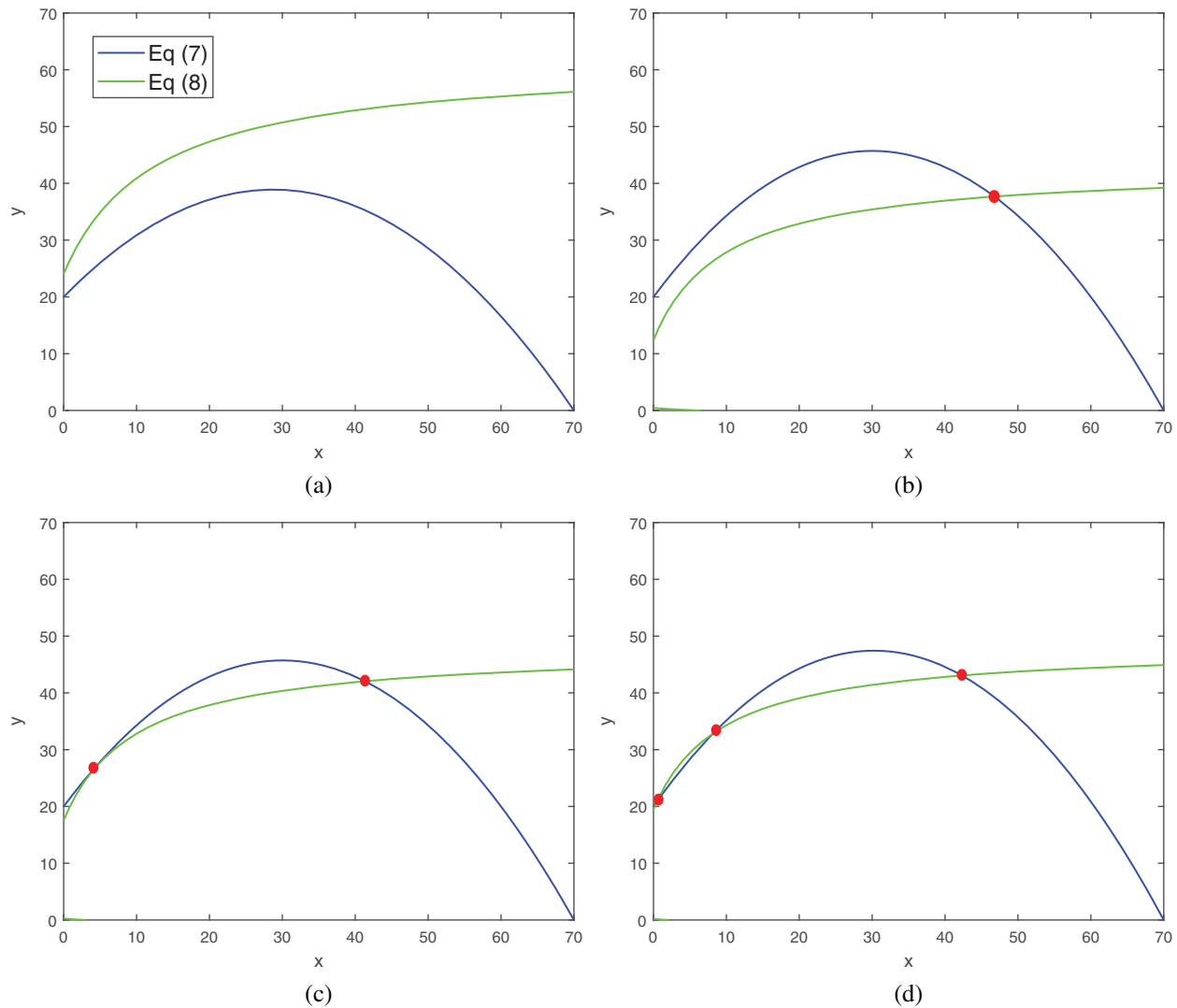


Figure 1: Four possibilities of the prey and predator zero growth isoclines. (a) Interior equilibrium does not exist for the parametric values $a=0.08$, $d=0.01$, (b) interior equilibrium exists uniquely for the values of parameters $a=0.1$, $d=0.235$, (c) two interior equilibria for parameter values $a=0.1$, $d=0.137$, (d) three interior equilibria for parameter values $a=0.105$, $d=0.1$. Rest of the parameters are same as that in (25)

- In order to analyze the local stability of unique interior equilibrium $E^*(x^*, A^*, y^*)$, we evaluate the Jacobian matrix at E^* and it is given by

$$J|_{E^*} = \begin{bmatrix} -\frac{rx^*}{K} + \frac{\alpha(1-A_0)ax^*y^*}{(1+ax^*)^2} & 0 & -\frac{\alpha(1-A_0)x^*}{1+ax^*} \\ 0 & -\frac{\lambda A_0 y^*}{A^*} & \lambda A_0 - \phi A^* \\ \frac{c_1 \alpha (1-A_0) y^*}{(1+ax^*)^2} & c_2 \phi y^* & -ey^* \end{bmatrix}$$

Characteristic equation corresponding to above matrix is given by

$$\Lambda^3 + A_1\Lambda^2 + A_2\Lambda + A_3 = 0, \tag{14}$$

where

$$A_1 = \frac{rx^*}{K} - \frac{\alpha(1 - A_0)ax^*y^*}{(1 + ax^*)^2} + \frac{\lambda A_0 y^*}{A^*} + ey^*,$$

$$A_2 = \frac{\lambda A_0 ey^{*2}}{A^*} - c_2\phi(\lambda A_0 - \phi A^*)y^* + \left(\frac{rx^*}{K} - \frac{\alpha(1 - A_0)ax^*y^*}{(1 + ax^*)^2}\right)(ey^*)$$

$$+ \frac{c_1\alpha^2(1 - A_0)^2x^*y^*}{(1 + ax^*)^3} + \left(\frac{rx^*}{K} - \frac{\alpha(1 - A_0)ax^*y^*}{(1 + ax^*)^2}\right)\left(\frac{\lambda A_0 y^*}{A^*}\right),$$

$$A_3 = -\left(-\frac{rx^*}{K} + \frac{\alpha(1 - A_0)ax^*y^*}{(1 + ax^*)^2}\right)\left[\frac{\lambda A_0 ey^{*2}}{A^*} - c_2\phi(\lambda A_0 - \phi A^*)y^*\right]$$

$$+ \frac{\alpha(1 - A_0)x^*}{1 + ax^*}\left[\frac{\lambda A_0 y^*}{A^*} \frac{c_1\alpha(1 - A_0)y^*}{(1 + ax^*)^2}\right].$$

Now using the Routh–Hurwitz criterion, all eigenvalues of $J|_{E^*}$ have negative real part iff

$$A_1 > 0, \quad A_3 > 0, \quad A_1A_2 > A_3. \tag{15}$$

Thus we can state the following theorem.

Theorem 3.4 The system (1) is stable in the neighborhood of its positive equilibrium iff inequalities in (15) hold.

It is also noted that inequalities in (15) hold if

$$\frac{r}{K} > \frac{\alpha(1 - A_0)ay^*}{(1 + ax^*)^2}, \quad \lambda A_0 < \phi A^*. \tag{16}$$

Infect, the above two conditions imply that $A_1 > 0$ and $A_3 > 0$. The third condition $A_1A_2 > A_3$ is also satisfied.

Remark. The system (1) is stable around its positive equilibrium E^* if inequalities in (16) hold.

In the following theorem we give a criterion for global asymptotic stability of interior equilibrium $E^*(x^*, A^*, y^*)$ of the system (1).

Theorem 3.5. The interior equilibrium $E^*(x^*, A^*, y^*)$ of the system (1) is globally asymptotically stable under the following conditions:

$$\frac{r}{K} > \frac{\alpha(1 - A_0)ay^*}{1 + ax^*}, \quad c_2\lambda^2 A_0^2 < 4\beta eA^*. \tag{17}$$

Proof. We Choose a suitable Lyapunov function about E^* as

$$V(x, A, y) = \left(x - x^* - x^* \ln \frac{x}{x^*}\right) + \frac{\gamma_1}{2}(A - A^*)^2 + \gamma_2 \left(y - y^* - y^* \ln \frac{y}{y^*}\right),$$

where γ_1 and γ_2 are positive constants, to be specified later. Now, differentiating V with respect to t along the solutions of system (1), we get

$$\begin{aligned} \frac{dV}{dt} &= \left(\frac{x-x^*}{x} \right) \frac{dx}{dt} + \gamma_1 (A-A^*) \frac{dA}{dt} + \gamma_2 \left(\frac{y-y^*}{y} \right) \frac{dy}{dt} \\ &= - \left[\frac{r}{K} - \frac{\alpha(1-A_0)ay^*}{(1+ax)(1+ax^*)} \right] (x-x^*)^2 - \gamma_1 (\beta + \phi y) (A-A^*)^2 - \gamma_2 e (y-y^*)^2 \\ &\quad + (\gamma_1 \lambda A_0 - \gamma_1 \phi A^* + \gamma_2 c_2 \phi) (A-A^*) (y-y^*) + \left[-\frac{\alpha(1-A_0)}{1+ax} + \frac{\gamma_2 c_1 \alpha (1-A_0)}{(1+ax)(1+ax^*)} \right] (x-x^*) (y-y^*). \end{aligned}$$

Choosing $\gamma_2 = \frac{1+ax^*}{c_1}$ and $\gamma_1 = \frac{\gamma_2 c_2}{A^*}$, we get

$$\begin{aligned} \frac{dV}{dt} &= - \left[\frac{r}{K} - \frac{\alpha(1-A_0)ay^*}{(1+ax)(1+ax^*)} \right] (x-x^*)^2 - \frac{(1+ax^*)c_2}{c_1 A^*} (\beta + \phi y) (A-A^*)^2 \\ &\quad - \frac{1+ax^*}{c_1} e (y-y^*)^2 + \frac{(1+ax^*)c_2}{c_1 A^*} \lambda A_0 (A-A^*) (y-y^*). \end{aligned}$$

Applying Sylvester criterion, $\frac{dV}{dt}$ is negative definite if conditions in (17) hold. Hence E^* is globally stable under conditions in (17).

3.3 Hopf-Bifurcation and Its Properties

Hopf-bifurcation is a local phenomenon where a system's stability switches and a periodic solution arises around its equilibrium point by varying a parameter. In system (1), the parameter A_0 seems crucial, therefore we analyze the Hopf-bifurcation by taking A_0 as bifurcation parameter, then we have some $A_0 = A_0^*$. The necessary and sufficient conditions for occurrence Hopf-bifurcation at $A_0 = A_0^*$ are

- (a) $A_1|_{A_0^*} > 0$, $A_3|_{A_0^*} > 0$,
- (b) $f(A_0^*) \equiv (A_1 A_2 - A_3)|_{A_0^*} = 0$,
- (c) $Re \left[\frac{d\Lambda_i}{dA_0} \right]_{A_0=A_0^*}$ is either positive or negative, where Λ_i , $i = 1, 2, 3$ are roots of Eq. (14).

From $A_1 A_2 - A_3 = 0$, we get an equation in A_0 and assume that it has at least one positive root A_0^* . Then for some $\varepsilon > 0$, there is an interval containing A_0^* , $(A_0^* - \varepsilon, A_0^* + \varepsilon)$ such that $A_0^* - \varepsilon > 0$ and $A_2 > 0$ for $A_0 \in (A_0^* - \varepsilon, A_0^* + \varepsilon)$. Thus, Eq. (14) cannot have any real positive root for $A_0 \in (A_0^* - \varepsilon, A_0^* + \varepsilon)$.

Therefore, at $A_0 = A_0^*$, Eq. (14) becomes

$$(\Lambda + A_1)(\Lambda^2 + A_2) = 0,$$

this gives us three roots

$$\Lambda_{1,2} = \pm i\rho, \quad \Lambda_3 = \mu,$$

where $\rho = \sqrt{A_2}$ and $\mu = -A_1$.

For $A_0 \in (A_0^* - \varepsilon, A_0^* + \varepsilon)$, roots can be taken as $\Lambda_{1,2} = k_1(A_0) \pm ik_2(A_0)$, $\Lambda_3 = -A_1(A_0)$.

Now, we have to verify the transversality condition. Differentiating Eq. (14) with respect to the bifurcation parameter A_0 , we obtain

$$\left[\frac{d\Lambda}{dA_0} \right]_{A_0=A_0^*} = - \left[\frac{\dot{A}_1 \Lambda^2 + \dot{A}_2 \Lambda + \dot{A}_3}{3\Lambda^2 + 2A_1 \Lambda + A_2} \right]_{\Lambda=i\sqrt{A_2}} = - \frac{\frac{dR}{dA_0}}{2(A_1^2 + A_2)} + i \left[\frac{\sqrt{A_2} \dot{A}_2}{2A_2} - \frac{A_1 \sqrt{A_2} \frac{dR}{dA_0}}{2A_2(A_1^2 + A_2)} \right],$$

where $R = A_1 A_2 - A_3$ and \dot{A}_i , $i = 1, 2, 3$ denote the derivative of A_i with respect to time. Thus

$$Re \left[\frac{d\Lambda_i}{dA_0} \right]_{A_0=A_0^*} = - \frac{\frac{dR}{dA_0}}{2(A_1^2 + A_2)}.$$

Thus, we can state the following theorem.

Theorem 3.6. The system undergoes Hopf-bifurcation near interior equilibrium $E^*(x^*, A^*, y^*)$ under the necessary and sufficient conditions (a), (b) and (c). Critical value of bifurcation parameter A_0 is given by the equation $f(A_0^*) = 0$.

In order to see the stability and direction of Hopf-bifurcation, we use center manifold theorem [34] and some concepts used in [41]. Now, consider the following transformation

$$x_1 = x - x^*, \quad x_2 = A - A^*, \quad x_3 = y - y^*.$$

Using this transformation, system (1) takes the following form

$$\dot{X} = M^* X + G(X), \tag{18}$$

where $X = (x_1, x_2, x_3)^T$,

$$M^* = \begin{bmatrix} -\frac{rx^*}{K} + \frac{\alpha(1-A_0)ax^*y^*}{(1+ax^*)^2} & 0 & -\frac{\alpha(1-A_0)x^*}{1+ax^*} \\ 0 & -\frac{\lambda A_0 y^*}{A^*} & \lambda A_0 - \phi A^* \\ \frac{c_1 \alpha(1-A_0)y^*}{(1+ax^*)^2} & c_2 \phi y^* & -ey^* \end{bmatrix},$$

$$G = \begin{bmatrix} m_1 \\ m_2 \\ m_3 \end{bmatrix} = \begin{bmatrix} -\frac{rx_1^2}{K} - \frac{\alpha(1-A_0)x_1 x_3}{1+ax_1} \\ -\phi x_2 x_3 \\ \frac{c_1 \alpha(1-A_0)x_1 x_3}{1+ax_1} + c_2 \phi x_2 x_3 - ex_3^2 \end{bmatrix}$$

Let v_1 and v_2 be the eigenvectors corresponding to eigenvalues $i\rho$ and μ of E^* at $A_0 = A_0^*$. Then v_1 and v_2 are given by

$$v_1 = \begin{bmatrix} -\rho^2 + i\left(\frac{\lambda A_0 y^*}{A^*} + ey^*\right)\rho + \frac{\lambda A_0 y^{*2} e}{A^*} - c_2 \phi y^* (\lambda A_0 - \phi A^*) \\ \frac{c_1 \alpha (1 - A_0) y^*}{(1 + ax^*)^2} (\lambda A_0 - \phi A^*) \\ \frac{c_1 \alpha (1 - A_0) y^*}{(1 + ax^*)^2} \left(\frac{\lambda A_0 y^*}{A^*} - i\rho\right) \end{bmatrix}$$

and

$$v_2 = \begin{bmatrix} \mu^2 + i\left(\frac{\lambda A_0 y^*}{A^*} + ey^*\right)\mu + \frac{\lambda A_0 y^{*2} e}{A^*} - c_2 \phi y^* (\lambda A_0 - \phi A^*) \\ \frac{c_1 \alpha (1 - A_0) y^*}{(1 + ax^*)^2} (\lambda A_0 - \phi A^*) \\ \frac{c_1 \alpha (1 - A_0) y^*}{(1 + ax^*)^2} \left(\frac{\lambda A_0 y^*}{A^*} - \mu\right) \end{bmatrix} = \begin{bmatrix} p_{13} \\ p_{23} \\ p_{33} \end{bmatrix} \text{ (say).}$$

Let

$$H = (Im(v_1), Re(v_1), v_2) = \begin{bmatrix} p_{11} & p_{12} & p_{13} \\ p_{21} & p_{22} & p_{23} \\ p_{31} & p_{32} & p_{33} \end{bmatrix}$$

where

$$p_{11} = \left(\frac{\lambda A_0 y^*}{A^*} + ey^*\right)\rho, \quad p_{12} = -\rho^2 + \frac{\lambda A_0 y^{*2} e}{A^*} - c_2 \phi y^* (\lambda A_0 - \phi A^*), \quad p_{21} = 0,$$

$$p_{22} = \frac{c_1 \alpha (1 - A_0) y^*}{(1 + ax^*)^2} (\lambda A_0 - \phi A^*), \quad p_{31} = -\frac{c_1 \alpha (1 - A_0) y^* \rho}{(1 + ax^*)^2}, \quad p_{32} = \frac{c_1 \alpha (1 - A_0) y^* \lambda A_0 y^*}{(1 + ax^*)^2 A^*}.$$

$$\text{Then } H^{-1} = \frac{1}{\Delta} \begin{bmatrix} q_{11} & q_{12} & q_{13} \\ q_{21} & q_{22} & q_{23} \\ q_{31} & q_{32} & q_{33} \end{bmatrix}, \text{ where}$$

$$\Delta = p_{11}(p_{22}p_{33} - p_{23}p_{32}) + p_{12}(p_{23}p_{31} - p_{21}p_{33}) + p_{13}(p_{21}p_{32} - p_{22}p_{31}) \neq 0,$$

$$q_{11} = p_{22}p_{33} - p_{23}p_{32}, \quad q_{12} = p_{21}p_{33} - p_{23}p_{31}, \quad q_{13} = p_{21}p_{32} - p_{22}p_{31},$$

$$q_{21} = p_{12}p_{33} - p_{13}p_{32}, \quad q_{22} = p_{11}p_{33} - p_{13}p_{31}, \quad q_{23} = p_{11}p_{32} - p_{31}p_{12},$$

$$q_{31} = p_{12}p_{23} - p_{13}p_{22}, \quad q_{32} = p_{11}p_{23} - p_{13}p_{21}, \quad q_{33} = p_{11}p_{22} - p_{12}p_{21}.$$

Now let $X = HY$ or $Y = H^{-1}X$, where $Y = (y_1, y_2, y_3)^T$. Using this transformation, system (18) can be written as

$$\dot{Y} = (H^{-1}M^*H)Y + F(Y), \tag{19}$$

where

$$F(Y) = H^{-1}G(HY) = \begin{bmatrix} f^1 \\ f^2 \\ f^3 \end{bmatrix} = \frac{1}{\Delta} \begin{bmatrix} q_{11}m_1 + q_{12}m_2 + q_{13}m_3 \\ q_{21}m_1 + q_{22}m_2 + q_{23}m_3 \\ q_{31}m_1 + q_{32}m_2 + q_{33}m_3 \end{bmatrix}, \quad H^{-1}M^*H = \begin{bmatrix} 0 & -\rho & 0 \\ \rho & 0 & 0 \\ 0 & 0 & \mu \end{bmatrix}.$$

So, we can write system (19) as

$$\begin{bmatrix} \dot{y}_1 \\ \dot{y}_2 \\ \dot{y}_3 \end{bmatrix} = \begin{bmatrix} 0 & -\rho & 0 \\ \rho & 0 & 0 \\ 0 & 0 & \mu \end{bmatrix} \begin{bmatrix} y_1 \\ y_2 \\ y_3 \end{bmatrix} + \begin{bmatrix} f^1 \\ f^2 \\ f^3 \end{bmatrix} \tag{20}$$

Thus, system (20) takes the following form

$$\begin{aligned} \dot{U} &= BU + f(U, V), \\ \dot{V} &= CU + g(U, V), \end{aligned} \tag{21}$$

where $U = (y_1, y_2)^T$, $V = (y_3)$, $B = \begin{bmatrix} 0 & -\rho \\ \rho & 0 \end{bmatrix}$, $C = (\mu)$, $f = (f^1, f^2)$ and $g = (f^3)$. The eigenvalues of B and C may have zero real part and negative real parts, respectively. f, g vanish along with their first partial derivative at the origin.

Since the center manifold is tangent to $W^C(y=0)$ we can represent it as a graph

$$W^C = \{(U, V) : V = h(U)\} : h(0) = h'(0) = 0,$$

where $h: U \rightarrow R^2$ is defined on some vicinity $U \subset R^2$ of the origin [42,43].

We consider the projection of vector field on $V = h(U)$ onto W^C :

$$\dot{U} = BU + f(U, V) = BU + f(U, h(U)). \tag{22}$$

Now we state the following theorem to approximate the center manifold.

Theorem 3.7. Let Φ be a C^1 mapping of a neighborhood of the origin in R^2 into R with $\Phi(0) = 0$ and $\Phi'(0) = 0$. If for some $q > 1$, $(N\Phi)(U) = o(|U|^q)$ as $U \rightarrow 0$, then $h(U) = \Phi(U) + o(|U|^q)$ as $U \rightarrow 0$, where

$$(N\Phi)(U) = \Phi'(U)[BU + f(U, \Phi(U))] - C\Phi(U) - g(U, \Phi(U)).$$

In order to approximate $h(U)$, we consider

$$y_3 = h(y_1, y_2) = \frac{1}{2}(b_{11}y_1^2 + 2b_{12}y_1y_2 + b_{22}y_2^2) + \text{h.o.t.}, \tag{23}$$

where h.o.t. stands for high order terms. Using (23), we get from (22)

$$\dot{y}_3 = \frac{\partial h}{\partial y_1} \frac{dy_1}{dt} + \frac{\partial h}{\partial y_2} \frac{dy_2}{dt} = \mu y_3 + f^3.$$

After simplification, we get

$$\left(\rho b_{12} - \frac{\mu}{2} b_{11}\right) y_1^2 + \left(-\rho b_{12} - \frac{\mu}{2} b_{22}\right) y_2^2 + \{\rho(-b_{11} + b_{22}) - \mu b_{12}\} y_1 y_2 = Q_1 y_1^2 + Q_2 y_1 y_2 + Q_3 y_2^2 + \text{h.o.t.}, \quad (24)$$

where

$$Q_1 = \frac{1}{\Delta} \left[q_{31} \left(-\frac{r}{K} p_{11}^2 - \alpha(1 - A_0) p_{11} p_{13} \right) + q_{32} (-\phi p_{21} p_{31}) + q_{33} (c_1 \alpha(1 - A_0) p_{11} p_{31} + c_2 \phi p_{21} p_{31} - e p_{31}^2) \right],$$

$$Q_2 = \frac{1}{\Delta} \left[q_{31} \left(-\frac{2r}{K} p_{11} p_{12} - \alpha(1 - A_0) (p_{11} p_{32} + p_{12} p_{31}) \right) + q_{32} (-\phi (p_{21} p_{32} + p_{31} p_{22})) \right. \\ \left. + q_{33} (c_1 \alpha(1 - A_0) (p_{11} p_{32} + p_{12} p_{31}) + c_2 \phi (p_{21} p_{32} + p_{22} p_{31}) - e p_{31} p_{32}) \right],$$

$$Q_3 = \frac{1}{\Delta} \left[q_{31} \left(-\frac{r}{K} p_{12}^2 - \alpha(1 - A_0) p_{12} p_{32} \right) + q_{32} (-\phi p_{32} p_{22}) + q_{33} (c_1 \alpha(1 - A_0) p_{12} p_{32} + c_2 \phi p_{22} p_{32} - e p_{32}^2) \right].$$

Equating both the sides of Eq. (24), we get

$$\rho b_{12} - \frac{\mu}{2} b_{11} = Q_1,$$

$$\rho(-b_{11} + b_{22}) - \mu b_{12} = Q_2,$$

$$-\rho b_{12} - \frac{\mu}{2} b_{22} = Q_3.$$

Using Cramer's rule,

$$b_{11} = -\frac{\rho^2(Q_1 + Q_3) + \frac{\mu}{2}(\rho Q_2 + \mu Q_1)}{\frac{\mu^3}{4} + \mu\rho^2},$$

$$b_{12} = -\frac{\frac{\mu^2}{4} Q_2 + \frac{\rho\mu}{2}(Q_3 - Q_1)}{\frac{\mu^3}{4} + \mu\rho^2},$$

$$b_{22} = -\frac{\frac{\mu^2}{2} Q_3 - \frac{\mu}{2} \rho Q_2 + \rho^2(Q_1 + Q_3)}{\frac{\mu^3}{4} + \mu\rho^2}.$$

We can find the behavior of the solution of system (21) from the following theorem.

Theorem 3.8. If the zero solution of (22) is stable (asymptotically stable/unstable), then the zero solution of (21) is also stable (asymptotically stable/unstable).

Now from Eq. (22), we have

$$\begin{bmatrix} \dot{y}_1 \\ \dot{y}_2 \end{bmatrix} = \begin{bmatrix} 0 & -\rho \\ \rho & 0 \end{bmatrix} \begin{bmatrix} y_1 \\ y_2 \end{bmatrix} + \begin{bmatrix} f^1 \\ f^2 \end{bmatrix}$$

where

$$f^1 = \frac{1}{\Delta}(q_{11}m_1 + q_{12}m_2 + q_{13}m_3), \quad f^2 = \frac{1}{\Delta}(q_{21}m_1 + q_{22}m_2 + q_{23}m_3),$$

$$m_1 = \left[-\frac{r}{K}p_{11}^2 - \alpha(1 - A_0)p_{11}p_{31} \right] y_1^2 + \left[-\frac{r}{K}p_{12}^2 - \alpha(1 - A_0)p_{12}p_{31} \right] y_2^2 \\ + \left[-\frac{2r}{K}p_{11}p_{12} - \alpha(1 - A_0)(p_{11}p_{32} + p_{12}p_{31}) \right] y_1y_2 + \text{h.o.t.},$$

$$m_2 = -\phi p_{21}p_{31}y_1^2 - \phi p_{22}p_{32}y_2^2 - \phi(p_{21}p_{32} + p_{22}p_{31})y_1y_2 + \text{h.o.t.},$$

$$m_3 = \left[c_1\alpha(1 - A_0)p_{11}p_{31} + c_2\phi p_{21}p_{31} - ep_{31}^2 \right] y_1^2 + \left[c_1\alpha(1 - A_0)p_{12}p_{32} + c_2\phi p_{22}p_{32} - ep_{32}^2 \right] y_2^2 \\ + [c_1\alpha(1 - A_0)(p_{11}p_{32} + p_{12}p_{31}) + c_2\phi(p_{21}p_{32} + p_{22}p_{31}) - 2ep_{31}p_{32}] y_1y_2 + \text{h.o.t.}$$

Let $f_{ij}^k = \left[\frac{\partial f^k}{\partial y_i \partial y_j} \right]_{(0,0)}$ and $f_{ijl}^k = \left[\frac{\partial f^k}{\partial y_i \partial y_j \partial y_l} \right]_{(0,0)}$. Therefore,

$$f_{11}^1 = \frac{2}{\Delta} \left[q_{11} \left[-\frac{r}{K}p_{11}^2 - \alpha(1 - A_0)p_{11}p_{31} \right] + q_{12}[-\phi p_{21}p_{31}] + q_{13} \left[c_1\alpha(1 - A_0)p_{11}p_{31} + c_2\phi p_{21}p_{31} - ep_{31}^2 \right] \right],$$

$$f_{11}^2 = \frac{2}{\Delta} \left[q_{21} \left[-\frac{r}{K}p_{11}^2 - \alpha(1 - A_0)p_{11}p_{31} \right] + q_{22}[-\phi p_{21}p_{31}] + q_{23} \left[c_1\alpha(1 - A_0)p_{11}p_{31} + c_2\phi p_{21}p_{31} - ep_{31}^2 \right] \right],$$

$$f_{22}^1 = \frac{2}{\Delta} \left[q_{11} \left[-\frac{r}{K}p_{12}^2 - \alpha(1 - A_0)p_{12}p_{31} \right] + q_{12}[-\phi p_{22}p_{32}] + q_{13} \left[c_1\alpha(1 - A_0)p_{12}p_{32} + c_2\phi p_{22}p_{32} - ep_{32}^2 \right] \right],$$

$$f_{22}^2 = \frac{2}{\Delta} \left[q_{21} \left[-\frac{r}{K}p_{12}^2 - \alpha(1 - A_0)p_{12}p_{31} \right] + q_{22}[-\phi p_{22}p_{32}] + q_{23} \left[c_1\alpha(1 - A_0)p_{12}p_{32} + c_2\phi p_{22}p_{32} - ep_{32}^2 \right] \right],$$

$$f_{12}^1 = \frac{1}{\Delta} \left[q_{11} \left[-\frac{2r}{K}p_{11}p_{12} - \alpha(1 - A_0)(p_{11}p_{32} + p_{12}p_{31}) \right] + q_{12}[-\phi(p_{21}p_{32} + p_{22}p_{31})] \right. \\ \left. + q_{13} [c_1\alpha(1 - A_0)(p_{11}p_{32} + p_{12}p_{31}) + c_2\phi(p_{21}p_{32} + p_{22}p_{31}) - 2ep_{31}p_{32}] \right],$$

$$f_{12}^2 = \frac{1}{\Delta} \left[q_{21} \left[-\frac{2r}{K}p_{11}p_{12} - \alpha(1 - A_0)(p_{11}p_{32} + p_{12}p_{31}) \right] + q_{22}[-\phi(p_{21}p_{32} + p_{22}p_{31})] \right. \\ \left. + q_{23} [c_1\alpha(1 - A_0)(p_{11}p_{32} + p_{12}p_{31}) + c_2\phi(p_{21}p_{32} + p_{22}p_{31}) - 2ep_{31}p_{32}] \right],$$

$$f_{111}^1 = \frac{6}{\Delta} \left[q_{11} \left(-\frac{r}{K} p_{11} p_{13} b_{11} - \alpha(1 - A_0) + \left(-ap_{11}^2 p_{31} + \frac{p_{11} p_{33} b_{11} + p_{13} p_{31} b_{11}}{2} \right) \right) \right. \\ \left. + q_{12} \left(-\frac{\phi}{2} (p_{21} p_{33} b_{11} + p_{23} p_{31} b_{11}) \right) + q_{13} \left(c_1 \alpha(1 - A_0) \left(-ap_{11}^2 p_{31} + \frac{p_{11} p_{33} b_{11} + p_{31} p_{31} b_{11}}{2} \right) \right) \right. \\ \left. + \frac{c_2 \phi}{2} (p_{21} p_{33} b_{11} + p_{31} p_{23} b_{11} - ep_{31} p_{33} b_{11}) \right],$$

$$f_{222}^2 = \frac{6}{\Delta} \left[q_{21} \left(-\frac{r}{K} p_{12} p_{13} b_{22} - \alpha(1 - A_0) + \left(-ap_{12}^2 p_{32} + \frac{p_{12} p_{33} b_{22} + p_{13} p_{32} b_{22}}{2} \right) \right) \right. \\ \left. + q_{22} \left(-\frac{\phi}{2} (p_{22} p_{33} b_{22} + p_{23} p_{32} b_{22}) \right) + q_{23} \left(c_1 \alpha(1 - A_0) \left(-ap_{12}^2 p_{32} + \frac{p_{12} p_{33} b_{22} + p_{32} p_{13} b_{22}}{2} \right) \right) \right. \\ \left. + \frac{c_2 \phi}{2} (p_{22} p_{33} b_{22} + p_{32} p_{23} b_{22} - ep_{32} p_{33} b_{22}) \right],$$

$$f_{122}^1 = \frac{1}{\Delta} \left[q_{11} \left(-\frac{r}{K} (2p_{11} p_{13} b_{22} + 4p_{12} p_{13} b_{12}) - \alpha(1 - A_0) \left(-4ap_{11} p_{32} b_{12} - 2ap_{12}^2 p_{31} + p_{11} p_{33} b_{22} + 2p_{12} p_{33} b_{12} \right) \right. \right. \\ \left. + p_{31} p_{13} b_{22} + 2p_{32} p_{13} b_{12} \right) + q_{12} (-\phi (p_{21} p_{33} b_{22} + 2p_{22} p_{33} b_{12} + p_{31} p_{23} b_{22} + 2p_{32} p_{23} b_{12})) \\ \left. + q_{13} \left(c_1 \alpha(1 - A_0) \left(-4ap_{11} p_{32} b_{12} - 2ap_{12}^2 p_{31} + p_{11} p_{33} b_{22} + 2p_{12} p_{33} b_{12} + p_{31} p_{13} b_{22} + 2p_{32} p_{13} b_{12} \right) \right) \right. \\ \left. + c_2 \phi (p_{21} p_{33} b_{22} + 2p_{22} p_{33} b_{12} + p_{31} p_{23} b_{22} + 2p_{32} p_{23} b_{12}) - e(2p_{31} p_{33} b_{22} + 4p_{32} p_{33} b_{12}) \right],$$

$$f_{112}^2 = \frac{1}{\Delta} \left[q_{21} \left(-\frac{r}{K} (2p_{12} p_{13} b_{11} + 4p_{11} p_{13} b_{12}) - \alpha(1 - A_0) \left(-4ap_{11} p_{31} b_{12} - 2ap_{11}^2 p_{32} + p_{12} p_{33} b_{11} + 2p_{11} p_{33} b_{12} \right) \right. \right. \\ \left. + p_{32} p_{13} b_{11} + 2p_{31} p_{13} b_{12} \right) + q_{22} (-\phi (p_{22} p_{33} b_{11} + 2p_{21} p_{33} b_{12} + p_{32} p_{23} b_{12} + 2p_{31} p_{23} b_{12})) \\ \left. + q_{23} \left(c_1 \alpha(1 - A_0) \left(-4ap_{11} p_{31} b_{12} - 2ap_{11}^2 p_{32} + p_{11} p_{33} b_{12} + 2p_{12} p_{33} b_{11} + p_{32} p_{13} b_{11} + 2p_{31} p_{13} b_{12} \right) \right) \right. \\ \left. + c_2 \phi (p_{22} p_{33} b_{11} + 2p_{21} p_{33} b_{12} + p_{32} p_{23} b_{11} + 2p_{31} p_{23} b_{12}) - e(2p_{32} p_{33} b_{11} + 4p_{31} p_{33} b_{12}) \right].$$

We determine the direction and stability of bifurcation periodic orbit of the system (21) by the following formula [44]

$$\nu \left[\frac{dK}{dA_0} \right]_{A_0=A_0^*} = \frac{1}{\rho} \left[f_{12}^1 (f_{11}^1 + f_{22}^1) - f_{12}^2 (f_{11}^2 + f_{22}^2) - f_{11}^1 f_{11}^2 + f_{22}^1 f_{22}^2 - (f_{111}^1 + f_{112}^2 + f_{122}^1 + f_{222}^2) \right].$$

In above expression, if $\nu > 0 (< 0)$, then the Hopf-bifurcation is supercritical (subcritical) and bifurcation periodic solution exists for $A_0 = A_0^*$. The bifurcating periodic solution is stable (unstable) if

$$\nu \left[\frac{dK}{dA_0} \right]_{A_0=A_0^*} > 0 (< 0).$$

The bifurcating direction of periodic solution of the system (1) is same as the system (21).

3.4 Numerical Simulation

To validate our theoretical findings of model (1), we perform some numerical simulations using MATLAB R2018b. We have chosen the following dataset

$$r = 3, \quad K = 70, \quad \alpha = 0.3, \quad a = 0.07, \quad A_0 = 0.5, \quad \lambda = 2, \\ \beta = 0.32, \quad \phi = 0.7, \quad c_1 = 0.4, \quad c_2 = 0.5, \quad d = 0.3, \quad e = 0.02. \tag{25}$$

For the above set of parameters, condition for existence of prey free equilibrium (5) and conditions for existence and uniqueness of interior equilibrium (9) and (10) are satisfied. Therefore, the system (1) has five equilibrium points. The behavior of these equilibrium points are given in Tab. 2.

Table 2: Existing equilibria and their stability nature

Equilibrium point	Eigenvalues	Stability nature
$E_0(0, 0, 0)$	3, -0.32, -0.3	Saddle point
$E_1(70, 0, 0)$	-3, -0.32, 0.4113	Saddle point
$\tilde{E}_2(0, 0.9019, 0.7828)$	0.0898, -0.9734, 2.8826	Saddle point
$\hat{E}_2(0, 1.3577, 8.7601)$	-0.1511, -6.4762, 1.6860	Saddle point
$E^*(18.0971, 1.4094, 33.6153)$	$-0.0990 \pm 0.3860i, -23.7585$	Locally asymptotically stable

The eigenvalues of the Jacobian matrix at E_0 and E_1 are $(3, -0.32, -0.3)$ and $(-3, -0.32, 0.4113)$, respectively. Therefore E_0 and E_1 both are saddle points. Similarly \tilde{E}_2 and \hat{E}_2 are also saddle points. Again all the inequalities in (15) are satisfied. So according to Theorem 3.4, the interior equilibrium E^* is locally asymptotically stable. The stability of system in the vicinity of the positive equilibrium E^* is illustrated by Fig. 2. In Fig. 2a, time evolution of species is shown and it is noted that they converge to their equilibrium levels after some oscillations. In Fig. 2b, phase diagram is drawn in xAy -space which shows the asymptotic stability behavior of positive equilibrium E^* .

In this study, we found that predators dependency factor A_0 on additional food plays an important role in the dynamics of the system. If it is less than a threshold value then it can be the cause of destabilizing the system. The threshold value can be calculated by solving $f(A_0^*) = 0$ (Theorem 3.6). By our computer simulation we obtain it as $A_0^* = 0.482$. All the conditions of Theorem 3.6 are satisfied, so the system undergoes a Hopf-bifurcation at $A_0^* = 0.482$. If we keep the value of parameter A_0 below its threshold value, then the system (1) always remains unstable. The instable behavior of solutions and presence of stable limit cycle at $A_0 = 0.45 < A_0^* = 0.482$ is shown in Fig. 3. In Fig. 4, we draw the bifurcation diagram with respect to parameter A_0 for both prey and predator species. From the figure, it is noted that the periodic solution present in the system when $A_0 \in [0, A_0^*]$ and oscillations can be removed from the system by increasing the parameter A_0 beyond A_0^* .

In the model (1), consumption rate of additional food ϕ is also a vital parameter. We have noted that if system is stable for parameter A_0 ($A_0 \in [0.482, 1]$) then it is stable for all range of parameter ϕ . But if $A_0 \in [0.2361, 0.482)$ then system undergoes a Hopf-bifurcation with respect to parameter ϕ . In Fig. 5, we have shown the bifurcation diagram when $A_0 = 0.4$ and other parameters are same as given in (25). The Hopf-bifurcation point is $\phi^* = 0.02847$.

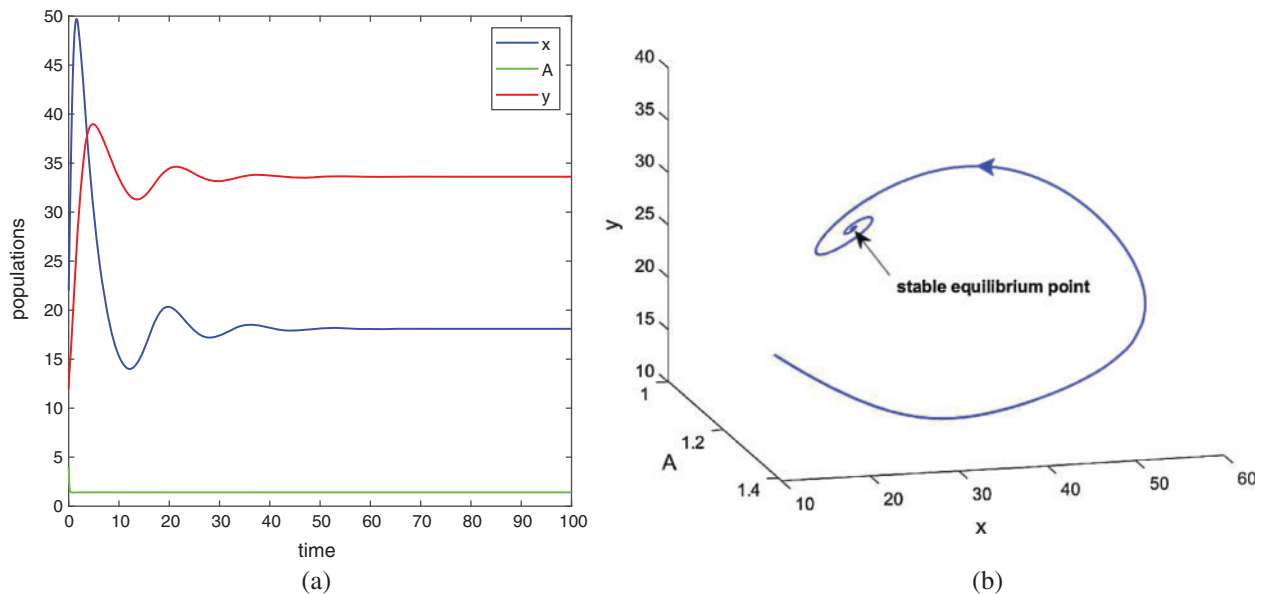


Figure 2: Time series evolution (a) and phase portrait (b) of species for the set of parameters chosen in (25). Positive equilibrium E^* is locally asymptotically stable

As the system (1) shows Hopf-bifurcation with respect to parameters A_0 and ϕ , and direction of Hopf-bifurcation is opposite for both the parameters. Therefore, we can divide the $A_0\phi$ -plane into two regions

Region of stability (green) $S_1 = \{(A_0, \phi) : \text{system (1) is locally asymptotically stable}\}$,

Region of instability (white) $S_2 = \{(A_0, \phi) : \text{system (1) is unstable}\}$.

Both the regions are drawn in Fig. 6. The curve which separates both the regions is called Hopf-bifurcation curve.

The number of interior equilibrium points depend on the values of parameters. In the table below, we have shown dependence of total number of interior equilibrium on parameters a and d and the nature of their stability. It is observed that when $a = 0.105$ and $d = 0.1$ (other parameters are as in (25)), then three interior equilibrium exist for the system (1), $E_1^*(0.5099, 1.398, 20.9174)$, $E_2^*(8.2355, 1.409, 32.9068)$ and $E_3^*(42.309, 1.4136, 43.0591)$. E_1^* and E_3^* are locally asymptotically stable and E_2^* is unstable. Since there are two locally asymptotically stable equilibrium in the system, so it shows bistability. Bistability is a phenomenon where a system converges to two different equilibrium points for the same parametric values based on the variation of the initial conditions. In Fig. 7, we initiated two trajectories from two nearby points and they converge to different interior equilibria. The black dotted curve is separatrix, which divides the xy -plane into two regions in such a way that if a solution is initiated from the left of the separatrix, it converges to E_1^* and if a solution is initiated from the right of the separatrix, it converges to E_3^* . In other words, left region is region of attraction for E_1^* and right region is region of attraction for E_3^* .

Remark. For the best representation of bistability phenomenon and separatrix curve, the Fig. 7 is drawn in the xy -plane. But initial conditions and interior equilibrium points are written as they are.

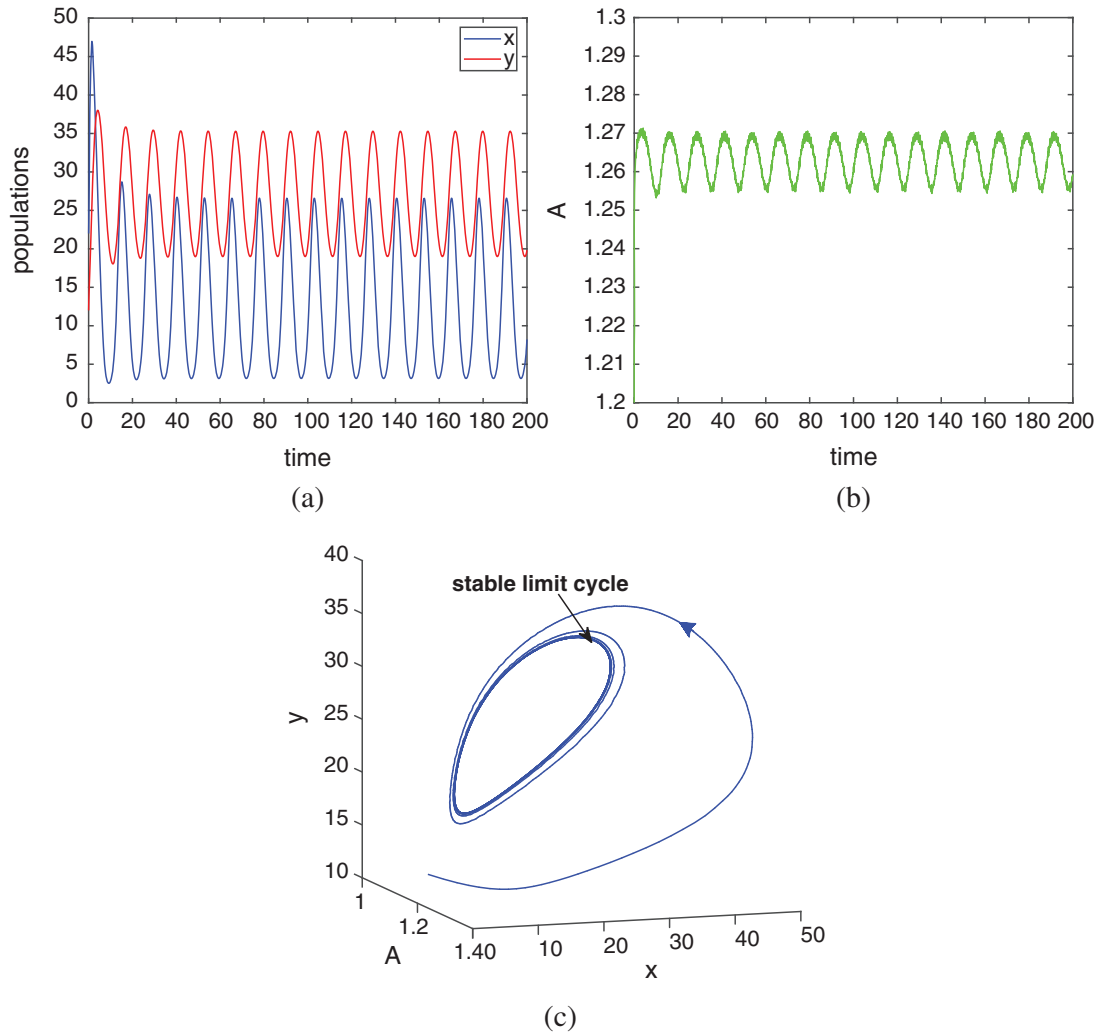


Figure 3: Instable behavior of solutions and existence of stable limit cycle for $A_0 = 0.45 (< A_0^*)$. Rest of the parameters are same as (25)

4 Analysis of Delayed Model

In this section, we discuss the local stability and Hopf-bifurcation phenomenon for the delayed system (2). The introduction of time delay does not affect the equilibria of the system. So, all the equilibria remain same as the non-delayed system (1). To see the effect of delay on the dynamical behavior of the interior equilibrium E^* , we rewrite the delayed system (2) as

$$\frac{dU(t)}{dt} = F(U(t), U(t - \tau_1), U(t - \tau_2)), \tag{26}$$

where

$$U(t) = [x(t), A(t), y(t)]^T, \quad U(t - \tau_1) = [x(t - \tau_1), A(t - \tau_1), y(t - \tau_1)]^T,$$

$$U(t - \tau_2) = [x(t - \tau_2), A(t - \tau_2), y(t - \tau_2)]^T.$$

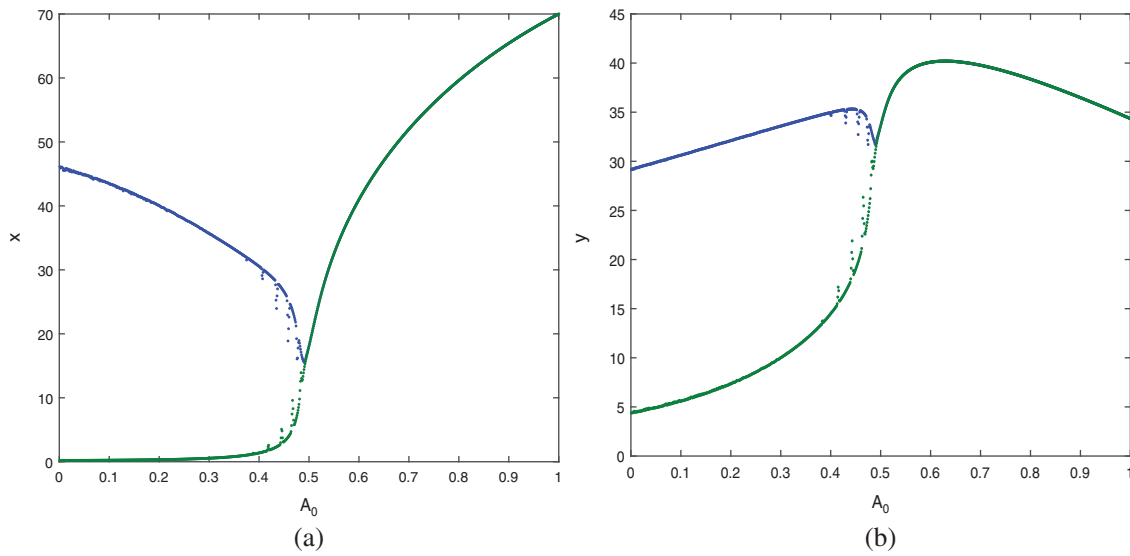


Figure 4: Bifurcation diagram of the prey and predator population with respect to parameter A_0

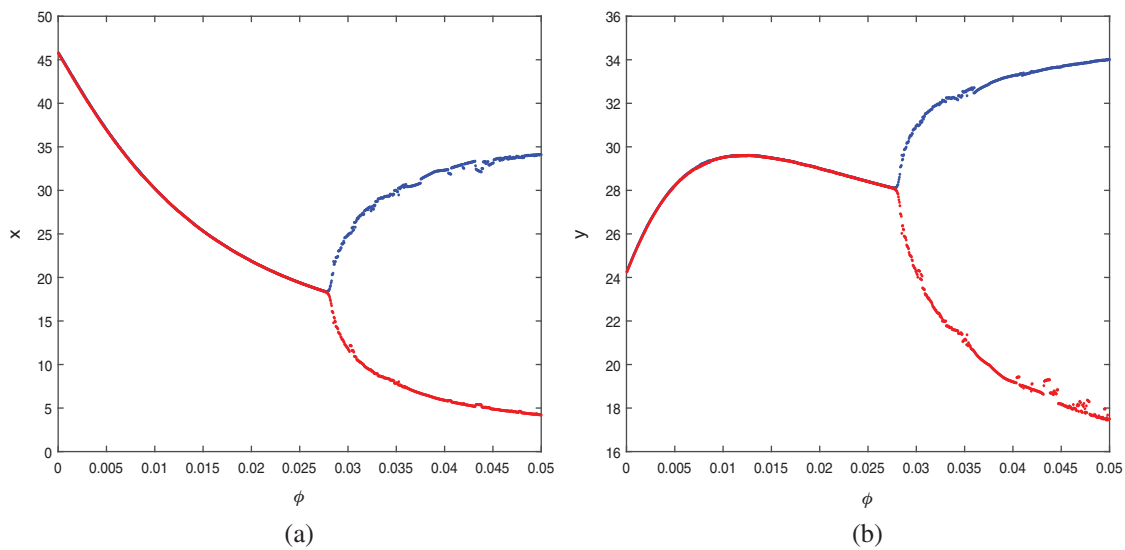


Figure 5: Bifurcation diagram of the prey and predator population with respect to parameter ϕ

Now we linearize the system (26) by using the following transformations:

$$x(t) = \bar{x}(t) + x^*, \quad A(t) = \bar{A}(t) + A^*, \quad y(t) = \bar{y}(t) + y^*,$$

where \bar{x} , \bar{A} and \bar{y} are small perturbations around x^* , A^* and y^* , respectively. Then the linearized system of (26) about the interior equilibrium E^* is given by

$$\frac{dZ}{dt} = PZ(t) + Q_1Z(t - \tau_1) + Q_2Z(t - \tau_2),$$

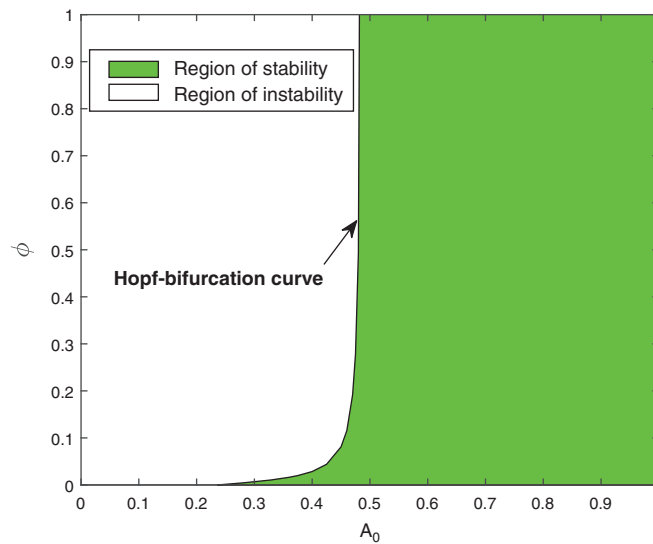


Figure 6: Region of stability and instability for system (1) in $A_0\phi$ -plane

Table 3: Dependence of total number of interior equilibria and their stability on parameters a and d . Rest of the parameters are same as in (25)

Parametric values	No. of interior equilibrium points	Equilibrium points	Nature of equilibrium points
$a = 0.08, d = 0.01$	0	–	–
$a = 0.1, d = 0.235$	1	(46.7827, 1.4114, 37.6669)	Stable
$a = 0.1, d = 0.137$	2	(4.4407, 1.4048, 27.0479)	Unstable
		(41.3432, 1.4132, 42.038)	Stable
$a = 0.105, d = 0.1$	3	(0.5099, 1.398, 20.9174)	Stable
		(8.2355, 1.409, 32.9068)	Unstable
		(42.309, 1.4136, 43.0591)	Stable

where

$$P = \left[\frac{\partial F}{\partial U(t)} \right]_{E^*}, \quad Q_1 = \left[\frac{\partial F}{\partial U(t - \tau_1)} \right]_{E^*}, \quad Q_2 = \left[\frac{\partial F}{\partial U(t - \tau_2)} \right]_{E^*}, \quad Z = [\bar{x}(t), \bar{A}(t), \bar{y}(t)]^T.$$

Thus, the Jacobian matrix of the system (2) at E^* is given by

$$\begin{bmatrix} a_1 & 0 & -a_2 \\ 0 & a_3 & a_4 \\ c_1 a_5 e^{-\xi \tau_1} & c_2 \phi y^* e^{-\xi \tau_2} & a_6 + c_1 a_2 e^{-\xi \tau_1} + c_2 \phi A^* e^{-\xi \tau_2} \end{bmatrix}$$

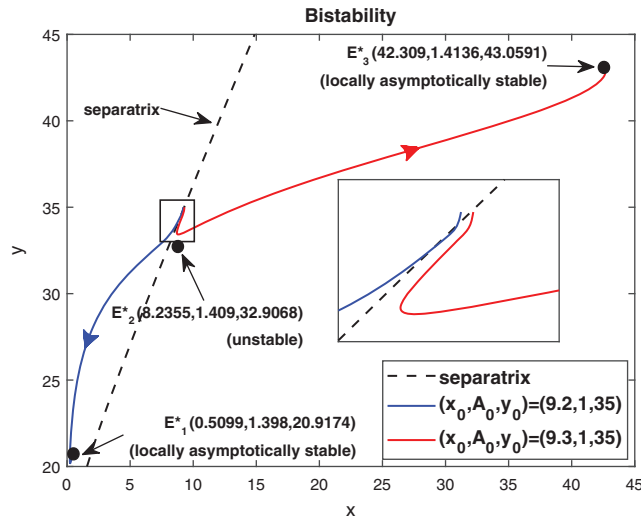


Figure 7: Trajectories initiated from region of attraction of both the locally asymptotically stable equilibrium points, system (1) shows bistability

where

$$a_1 = r - \frac{2rx^*}{K} - \frac{\alpha(1-A_0)y^*}{(1+ax^*)^2}, \quad a_2 = \frac{\alpha(1-A_0)x^*}{1+ax^*}, \quad a_3 = -\beta - \phi y^*, \quad a_4 = \lambda A_0 - \phi A^*,$$

$$a_5 = \frac{\alpha(1-A_0)y^*}{(1+ax^*)^2}, \quad a_6 = -d - 2ey^*.$$

The characteristic equation corresponding to the above Jacobian matrix is

$$\xi^3 + b_1\xi^2 + b_2\xi + b_3 + (b_4\xi^2 + b_5\xi + b_6)e^{-\xi\tau_1} + (b_7\xi^2 + b_8\xi + b_9)e^{-\xi\tau_2} = 0, \quad (27)$$

where

$$b_1 = -(a_1 + a_3 + a_6), \quad b_2 = a_3a_6 + a_1a_6 + a_1a_3, \quad b_3 = -a_1a_3a_6, \quad b_4 = -c_1a_2,$$

$$b_5 = c_1a_2(a_1 + a_3 + a_5), \quad b_6 = -c_1a_2a_3(a_1 + a_2), \quad b_7 = -c_2\phi A^*, \quad b_8 = c_2\phi(a_1A^* + a_3A^* - a_4y^*),$$

$$b_9 = c_2a_1\phi(-a_3A^* + a_4y^*).$$

Remark. When $\tau_1 = \tau_2 = 0$, then the characteristic Eq. (27) is same as the characteristic Eq. (14) for non-delayed system.

Case (1): $\tau_1 > 0$, $\tau_2 = 0$. Then Eq. (27) becomes

$$\xi^3 + d_1\xi^2 + d_2\xi + d_3 + (b_4\xi^2 + b_5\xi + b_6)e^{-\xi\tau_1} = 0, \quad (28)$$

where

$$d_1 = b_1 + b_7, \quad d_2 = b_2 + b_8, \quad d_3 = b_3 + b_9.$$

For the delayed system (2), the positive equilibrium is locally asymptotically stable if and only if all the roots of the Eq. (28) have negative real parts. For switching of the stability, the root of

the Eq. (28) must cross the imaginary axis. Therefore let $i\omega(\omega > 0)$ be a root of Eq. (28), then it follows that

$$\begin{aligned} (-b_4\omega^2 + b_6) \cos(\omega\tau_1) + b_5\omega \sin(\omega\tau_1) &= d_1\omega^2 - d_3, \\ b_5\omega \cos(\omega\tau_1) - (-b_4\omega^2 + b_6) \sin(\omega\tau_1) &= \omega^3 - d_2\omega. \end{aligned} \tag{29}$$

From the above set of equations, we can obtain

$$\omega^6 + h_1\omega^4 + h_2\omega^2 + h_3 = 0, \tag{30}$$

where

$$h_1 = d_1^2 - b_4^2 - 2d_2, \quad h_2 = d_2^2 - b_5^2 - 2d_1d_3 + 2b_4b_6, \quad h_3 = d_3^2 - b_6^2.$$

If we put $\omega^2 = z$, then Eq. (30) becomes

$$g(z) = z^3 + h_1z^2 + h_2z + h_3 = 0. \tag{31}$$

Theorem 4.1. If Eq. (31) has no positive root, then there is no change in the stability behavior of E^* for all $\tau_1 \geq 0$.

Corollary. If inequalities in (15) hold and Eq. (31) has no positive root, then E^* is locally asymptotically stable for all $\tau_1 \geq 0$.

Corollary. If inequalities in (15) do not hold and Eq. (31) has no positive root, then E^* is unstable for all $\tau_1 \geq 0$.

Now let inequalities in (15) hold and Eq. (31) has at least one positive root, say $z_1 = \omega_1^2$. Substituting ω_1 into Eq. (29), we obtain

$$\tau_{1_i} = \frac{1}{\omega_1} \cos^{-1} \left[\frac{(d_1\omega_1^2 - d_3)(-b_4\omega_1^2 + b_6) + (\omega_1^3 - d_2\omega_1)\omega_1 b_5}{(-b_4\omega_1^2 + b_6)^2 + \omega_1^2 b_5^2} \right] + \frac{2i\pi}{\omega_1}, \quad i = 0, 1, 2, \dots \tag{32}$$

$$(H_1) : g'(\omega_1^2) > 0.$$

Let $\xi(\tau_{1_i}) = \pm i\omega_1$ be the root of Eq. (28), a little calculation yields

$$Re \left[\frac{d\xi}{d\tau_1} \right]_{\xi=i\omega_1, \tau_1=\tau_{1_i}}^{-1} = \frac{g'(\omega_1^2)}{(-b_4\omega_1^2 + b_6)^2 + \omega_1^2 b_5^2} > 0.$$

But sign of $\left[\frac{d}{d\tau_1} Re(\xi) \right]_{\xi=i\omega_1, \tau_1=\tau_{1_i}}$ is same as the sign of $\left[Re \left(\frac{d\xi}{d\tau_1} \right) \right]_{\xi=i\omega_1, \tau_1=\tau_{1_i}}$.

Hence, the transversality condition can be obtained under (H_1)

$$\left[\frac{d}{d\tau_1} (Re(\xi)) \right]_{\tau_1=\tau_{1_i}} > 0,$$

Thus, we can state the following theorem.

Theorem 4.2. For system (2), with $\tau_2 = 0$ and assuming that (H_1) holds, there exists a positive number τ_{10} such that the equilibrium E^* is locally asymptotically stable when $\tau_1 < \tau_{10}$ and unstable when $\tau_1 > \tau_{10}$. Furthermore system (2) undergoes a Hopf-bifurcation at E^* when $\tau_1 = \tau_{10}$.

Case (2): $\tau_1 = 0, \tau_2 > 0$. Then Eq. (27) becomes

$$\xi^3 + e_1\xi^2 + e_2\xi + e_3 + (b_7\xi^2 + b_8\xi + b_9)e^{-\xi\tau_2} = 0, \quad (33)$$

where

$$e_1 = b_1 + b_4, \quad e_2 = b_2 + b_5, \quad e_3 = b_3 + b_6.$$

Under an analysis similar to Case (1), one can easily deduce the following theorem.

Theorem 4.3. For $\tau_1 = 0$, the interior equilibrium point is locally asymptotically stable for $\tau_2 < \tau_{20}$, unstable for $\tau_2 > \tau_{20}$, and it undergoes Hopf-bifurcation at $\tau_2 = \tau_{20}$ given by

$$\tau_{20} = \frac{1}{\omega_2} \cos^{-1} \left[\frac{(e_1\omega_2^2 - e_3)(-b_7\omega_2^2 + b_9) + (\omega_2^3 - e_2\omega_2)\omega_2 b_8}{(-d_7\omega_2^2 + b_9)^2 + \omega_2^2 b_8^2} \right],$$

where $i\omega_2$ is root of characteristic Eq. (33).

Case (3): τ_1 is fixed in the interval $(0, \tau_{10})$ and assuming τ_2 as a variable parameter.

We consider Eq. (27) with τ_1 as fixed in its stable interval $(0, \tau_{10})$ and τ_2 as a variable. Let $i\omega$ ($\omega > 0$) be a root of characteristic Eq. (27). Then separating real and imaginary parts, we obtain

$$-b_1\omega^2 + b_3 + (-b_4\omega^2 + b_6)\cos(\omega\tau_1) + b_5\omega\sin(\omega\tau_1) = -(-b_7\omega^2 + b_9)\cos(\omega\tau_2) - b_8\omega\sin(\omega\tau_2), \quad (34)$$

$$-\omega^3 + b_2\omega - (-b_4\omega^2 + b_6)\sin(\omega\tau_1) + b_5\omega\cos(\omega\tau_1) = (-b_7\omega^2 + b_9)\sin(\omega\tau_2) - b_8\omega\cos(\omega\tau_2). \quad (35)$$

Squaring and then adding (34) and (35) to eliminate τ_2 , we obtain

$$\begin{aligned} & (-b_1\omega^2 + b_3)^2 + (-\omega^3 + b_2\omega)^2 + (-b_4\omega^2 + b_6)^2 + b_5^2\omega^2 \\ & + 2[(-b_1\omega^2 + b_3)(-b_4\omega^2 + b_6) + (-\omega^3 + b_2\omega)b_5\omega]\cos(\omega\tau_1) \\ & + 2[-(-\omega^3 + b_2\omega)(-b_4\omega^2 + b_6) + (-b_1\omega^2 + b_3)b_5\omega]\sin(\omega\tau_1) = (-b_7\omega^2 + b_9)^2 + b_8^2\omega^2. \end{aligned} \quad (36)$$

Eq. (36) is a transcendental equation in complex form. So, it is not easy to predict the nature of roots. Without going detailed analysis with (36), it is assumed that there exist at least one positive root ω_0 . Eqs. (34) and (35) can be re-written as

$$-(-b_7\omega_0^2 + b_9)\cos(\omega_0\tau_2) - b_8\omega_0\sin(\omega_0\tau_2) = D_1 \quad (37)$$

$$(-b_7\omega_0^2 + b_9)\sin(\omega_0\tau_2) - b_8\omega_0\cos(\omega_0\tau_2) = D_2 \quad (38)$$

where

$$D_1 = -b_1\omega_0^2 + b_3 + (-b_4\omega_0^2 + b_6)\cos(\omega_0\tau_1) + b_5\omega_0\sin(\omega_0\tau_1),$$

$$D_2 = -\omega_0^3 + b_2\omega_0 - (-b_4\omega_0^2 + b_6)\sin(\omega_0\tau_1) + b_5\omega_0\cos(\omega_0\tau_1).$$

Eqs. (37) and (38) lead to

$$\tau'_{2n} = \frac{1}{\omega_0} \cos^{-1} \left[\frac{-(-b_7\omega_0^2 + b_9)D_1 - b_8\omega_0 D_2}{(-b_7\omega_0^2 + b_9)^2 + b_8^2\omega_0^2} \right] + \frac{2n\pi}{\omega_0}, \quad n = 0, 1, 2, \dots \tag{39}$$

Now, to verify the transversality condition of Hopf-bifurcation, differentiating equation (34) and (35) with respect to τ_2 and substitute $\tau_2 = \tau'_{2_0}$, we obtain

$$\begin{aligned} P \left[\frac{d(Re \xi)}{d\tau_2} \right]_{\tau_2=\tau_2^*} + Q \left[\frac{d\omega_0}{d\tau_2} \right]_{\tau_2=\tau_2^*} &= R, \\ -Q \left[\frac{d(Re \xi)}{d\tau_2} \right]_{\tau_2=\tau_2^*} + P \left[\frac{d\omega_0}{d\tau_2} \right]_{\tau_2=\tau_2^*} &= S, \end{aligned} \tag{40}$$

where

$$\begin{aligned} P &= -3\omega_0^2 + b_2 + b_5 \cos(\omega_0\tau_1) - (-b_4\omega_0^2 + b_6)\tau_1 \cos(\omega_0\tau_1) + 2b_4\omega_0 \sin(\omega_0\tau_1) - b_5\omega_0\tau_1 \sin(\omega_0\tau_1) \\ &\quad - (-b_7\omega_0^2 + b_9)\tau_2 \cos(\omega_0\tau_2) + b_8 \cos(\omega_0\tau_2) - b_8\omega_0\tau_2 \sin(\omega_0\tau_2) + 2b_7\omega_0 \sin(\omega_0\tau_2), \end{aligned}$$

$$\begin{aligned} Q &= -2b_1\omega_0 - 2b_4\omega_0 \cos(\omega_0\tau_1) - (-b_4\omega_0^2 + b_6)\tau_1 \sin(\omega_0\tau_1) + b_5 \sin(\omega_0\tau_1) + b_5\omega_0 \cos(\omega_0\tau_1) \\ &\quad - 2b_7\omega_0 \cos(\omega_0\tau_2) - (-b_7\omega_0^2 + b_9)\tau_2 \sin(\omega_0\tau_2) - b_8\omega_0\tau_2 \cos(\omega_0\tau_2) + b_8 \sin(\omega_0\tau_2), \end{aligned}$$

$$R = (-b_7\omega_0^2 + b_9)\omega_0 \sin(\omega_0\tau_2) - b_8\omega_0^2 \cos(\omega_0\tau_2),$$

$$S = (-b_7\omega_0^2 + b_9)\omega_0 \cos(\omega_0\tau_2) + b_8\omega_0^2 \sin(\omega_0\tau_2).$$

Solving Eq. (40) for $\left[\frac{d(Re \xi)}{d\tau_2} \right]_{\tau_2=\tau'_{2_0}}$, it is obtained

$$\left[\frac{d(Re \xi)}{d\tau_2} \right]_{\tau_2=\tau'_{2_0}, \xi=i\omega_0} = \frac{PR - QS}{P^2 + Q^2}.$$

(H₂): $PR - QS \neq 0$.

Theorem 4.4. For system (2), with $\tau_1 \in (0, \tau_{1_0})$ and assuming that (H₂) holds, there exists a positive number τ'_{2_0} such that E^* is locally asymptotically stable when $\tau_2 < \tau'_{2_0}$ and unstable when $\tau_2 > \tau'_{2_0}$. Furthermore, system (2) undergoes a Hopf-bifurcation at E^* where $\tau_2 = \tau'_{2_0}$.

Case (4): τ_2 is fixed in the interval $(0, \tau_{2_0})$ and assuming τ_1 as a variable parameter Under an analysis similar to Case (3), one can easily prove the following theorem.

Theorem 4.5. For $\tau_2 \in (0, \tau_{2_0})$, the interior equilibrium point is locally asymptotically stable for $\tau_1 < \tau'_{1_0}$ and it undergoes Hopf-bifurcation at $\tau_1 = \tau'_{1_0}$, given by

$$\tau'_{1_0} = \frac{1}{\omega_*} \cos^{-1} \left[\frac{-(-b_4\omega_*^2 + b_6)D_3 - b_5\omega_* D_4}{(-b_4\omega_*^2 + b_6)^2 + b_5^2\omega_*^2} \right],$$

where

$$D_3 = -b_1\omega_*^2 + b_3 + (-b_7\omega_*^2 + b_9)\cos(\omega_*\tau_2) + b_8\omega_*\sin(\omega_*\tau_2),$$

$$D_4 = -\omega_*^3 + b_2\omega_* - (-b_7\omega_*^2 + b_9)\sin(\omega_*\tau_2) + b_8\omega_*\cos(\omega_*\tau_2),$$

and $i\omega_*$ is characteristic root of Eq. (27).

5 Direction and Stability of Hopf-Bifurcation

Now with the help of center manifold theory and normal form concept (see [34] for details), we shall study direction and stability of the bifurcated periodic solutions at $\tau_1 = \tau'_{1_0}$.

Without loss of generality, we assume that $\tau_2^* < \tau'_{1_0}$, where $\tau_2^* \in (0, \tau_{2_0})$. Let

$$x_1(t) = x(t) - x^*, \quad A_1(t) = A(t) - A^*, \quad y_1(t) = y(t) - y^*,$$

and still denote $x_1(t)$, $A_1(t)$, $y_1(t)$ by $x(t)$, $A(t)$, $y(t)$. Let $\tau_1 = \tau'_{1_0} + \mu$, $\mu \in \mathbb{R}$ so that Hopf-bifurcation occurs at $\mu = 0$. We normalize the delay with scaling $t \mapsto (\frac{t}{\tau_1})$, then system (2) can be re-written as

$$\dot{U}(t) = \tau_1 \left(PU(t) + Q_1 U(t-1) + Q_2 U\left(t - \frac{\tau_2^*}{\tau_1}\right) + f(x, A, y) \right), \quad (41)$$

where $U(t) = (x(t), A(t), y(t))^T$,

$$P = \begin{bmatrix} a_1 & 0 & -a_2 \\ 0 & a_3 & a_4 \\ 0 & 0 & a_6 \end{bmatrix}, \quad Q_1 = \begin{bmatrix} 0 & 0 & 0 \\ 0 & 0 & 0 \\ c_1 a_5 & 0 & c_1 a_2 \end{bmatrix}, \quad Q_2 = \begin{bmatrix} 0 & 0 & 0 \\ 0 & 0 & 0 \\ 0 & c_2 \phi y^* & c_2 \phi A^* \end{bmatrix}, \quad f(x, A, y) = \begin{bmatrix} f_1 \\ f_2 \\ f_3 \end{bmatrix}$$

The nonlinear term f_1 , f_2 and f_3 are given by

$$f_1 = \left(-\frac{2r}{K} + \frac{2a\alpha(1-A_0)y^*}{(1+ax^*)^3} \right) x^2(t) - \frac{\alpha(1-A_0)}{(1+ax^*)^2} x(t)y(t) + \text{h.o.t.},$$

$$f_2 = -\phi A(t)y(t) + \text{h.o.t.},$$

$$f_3 = -2ey^2(t) - \frac{2c_1\alpha(1-A_0)y^*}{(1+ax^*)^3} x^2(t-1) + \frac{c_1\alpha(1-A_0)}{(1+ax^*)^2} x(t-1)y(t-1) \\ + c_2\phi A\left(t - \frac{\tau_2^*}{\tau_1}\right) y\left(t - \frac{\tau_2^*}{\tau_1}\right) + \text{h.o.t.},$$

The linearization of Eq. (41) around the origin is given by

$$\dot{U}(t) = \tau_1 (PU(t) + Q_1 U(t-1)) + Q_2 U\left(t - \frac{\tau_2^*}{\tau_1}\right).$$

For $\chi = (\chi_1, \chi_2, \chi_3)^T \in C([-1, 0], R^3)$, define

$$L_\mu(\chi) = (\tau_1 + \mu) (P\chi(0) + Q_1\chi(-1)) + Q_2\chi\left(-\frac{\tau_2^*}{\tau_1}\right).$$

By the Riesz representation theorem, there exists a 3×3 matrix $\eta(\theta, \mu)$, $(-1 \leq \theta \leq 0)$ whose element are of bounded variation function such that

$$L_\mu(\chi) = \int_{-1}^0 d\eta(\theta, \mu)\chi(\theta) \quad \text{for } \chi \in C([-1, 0], R^3). \tag{42}$$

In fact, we can obtain

$$\eta(\theta, \mu) = \begin{cases} (\tau'_{10} + \mu)(P + Q_1 + Q_2), & \text{if } \theta = 0 \\ (\tau'_{10} + \mu)(Q_1 + Q_2), & \text{if } \theta \in \left[-\frac{\tau_2^*}{\tau_1}, 0\right) \\ (\tau'_{10} + \mu)Q_2, & \text{if } \theta \in \left(-1, -\frac{\tau_2^*}{\tau_1}\right) \\ 0, & \text{if } \theta = -1. \end{cases}$$

Then Eq. (42) is satisfied.

For $\chi \in C^1([-1, 0], R^3)$, define the operator $H(\mu)$ as

$$H(\mu)\chi(\theta) = \begin{cases} \frac{d\chi(\theta)}{d\theta}, & \text{if } \theta \in [-1, 0) \\ \int_{-1}^0 [d\eta(\xi, \mu)]\chi(\xi), & \text{if } \theta = 0, \end{cases}$$

and

$$R(\mu)\chi(\theta) = \begin{cases} 0, & \text{if } \theta \in [-1, 0) \\ h(\mu, \chi), & \text{if } \theta = 0, \end{cases}$$

where

$$h(\mu, \chi) = (\tau'_{10} + \mu) \begin{bmatrix} h_1 \\ h_2 \\ h_3 \end{bmatrix}, \quad \chi = (\chi_1, \chi_2, \chi_3)^T \in C([-1, 0], R^3),$$

$$h_1 = \left(-\frac{2r}{K} + \frac{2a\alpha(1 - A_0)y^*}{(1 + ax^*)^3}\right)x^2(0) - \frac{\alpha(1 - A_0)}{(1 + ax^*)^2}x(0)y(0) + \text{h.o.t.},$$

$$h_2 = -\phi A(0)y(0) + \text{h.o.t.},$$

$$h_3 = -2ey^2(0) - \frac{2c_1\alpha(1 - A_0)y^*}{(1 + ax^*)^3}x^2(-1) + \frac{c_1\alpha(1 - A_0)}{(1 + ax^*)^2}x(-1)y(-1) + c_2\phi A\left(-\frac{\tau_2^*}{\tau'_{10}}\right)y\left(-\frac{\tau_2^*}{\tau'_{10}}\right) + \text{h.o.t.},$$

Then system (2) is equivalent to the following operator equation

$$\dot{U}_t = H(\mu)U_t + R(\mu)U_t,$$

where $U_t = U(t + \theta)$ for $\theta \in [-1, 0]$.

For $\psi \in C^1([0, 1], (R^3)^*)$, define

$$H^*\psi(s) = \begin{cases} -\frac{d\psi(s)}{ds}, & \text{if } s \in (0, 1] \\ \int_{-1}^0 \psi(-\xi)d\eta(\xi, 0), & \text{if } s = 0, \end{cases}$$

and a bilinear form

$$\langle \psi(s), \chi(\theta) \rangle = \bar{\psi}(0)\chi(0) - \int_{-1}^0 \int_{\xi=0}^{\theta} \bar{\psi}(\xi - \theta)d\eta(\theta)\chi(\xi)d\xi,$$

where $\eta(\theta) = \eta(\theta, 0)$, $H = H(0)$ and H^* are adjoint operators. From the discussion in previous section, we know that $\pm i\omega_0\tau'_{10}$ are the eigenvalues of $H(0)$ and therefore they are also eigenvalues of H^* . It is not difficult to verify that the vectors $q(\theta) = (1, \alpha_1, \beta_1)^T e^{i\omega_0\tau'_{10}\theta}$ ($\theta \in [-1, 0]$) and $q^*(s) = \frac{1}{D}(1, \alpha_1^*, \beta_1^*)e^{i\omega_0\tau'_{10}s}$ ($s \in [0, 1]$) are the eigenvectors of $H(0)$ and H^* corresponding to the eigenvalue $i\omega_0\tau'_{10}$ and $-i\omega_0\tau'_{10}$ respectively, where

$$\langle q^*(s), q(\theta) \rangle = 1, \quad \langle q^*(s), \bar{q}(\theta) \rangle = 1,$$

$$\beta_1 = \frac{c_1 a_5 e^{-i\omega_0\tau'_{10}}}{i\omega_0 - a_6 - c_1 a_2 e^{-i\omega_0\tau'_{10}} - c_2 \phi A^* e^{-i\omega_0 \frac{\tau_2^*}{\tau'_{10}}}}, \quad \alpha_1 = \frac{a_4 \beta_1}{i\omega_0 - a_3},$$

$$\beta_1^* = -\frac{i\omega_0 + a_1}{c_1 a_5 e^{-i\omega_0\tau'_{10}}}, \quad \alpha_1^* = \frac{a_2 - \left[i\omega_0 + a_6 + c_1 a_2 e^{-i\omega_0\tau'_{10}} + c_2 \phi A^* e^{-i\omega_0 \frac{\tau_2^*}{\tau'_{10}}} \right] \beta_1^*}{a_4},$$

$$D = \left[1 + \alpha_1 \bar{\alpha}_1^* + \beta_1 \bar{\beta}_1^* + \tau'_{10} \left(\bar{\beta}_1^* c_1 a_5 + \beta_1 \bar{\beta}_1^* c_1 a_2 \right) e^{-i\omega_0\tau'_{10}} + \tau_2^* \left(\alpha_1 \bar{\beta}_1^* c_2 \phi y^* + \beta_1 \bar{\beta}_1^* c_2 \phi A^* \right) e^{-i\omega_0 \frac{\tau_2^*}{\tau'_{10}}} \right].$$

Following the algorithms explained in Hassard et al. [34] and using a computation process similar to that in Song et al. [26], which is used to obtain the properties of Hopf-bifurcation, we obtain

$$g_{20} = -\frac{2\tau'_{10}}{D} \left[\frac{r}{K} + \beta_1 \alpha (1 - A_0) + \bar{\alpha}_1^* \phi \alpha_1 \beta_1 + \bar{\beta}_1^* e \beta_1^2 - \bar{\beta}_1^* c_1 \alpha (1 - A_0) \beta_1 e^{-2i\omega_0\tau'_{10}} - \bar{\beta}_1^* c_2 \phi \alpha_1 \beta_1 e^{-2i\omega_0\tau_2^*} \right],$$

$$g_{11} = -\frac{\tau'_{10}}{D} \left[2\frac{r}{K} + \alpha(1 - A_0)(\beta_1 + \bar{\beta}_1) + \bar{\alpha}_1^* \phi (\alpha_1 \bar{\beta}_1 + \bar{\alpha}_1 \beta_1) + 2\bar{\beta}_1^* e \beta_1 \bar{\beta}_1 - \bar{\beta}_1^* c_1 \alpha (1 - A_0)(\beta_1 + \bar{\beta}_1) + \bar{\beta}_1^* c_2 \phi (\alpha_1 \bar{\beta}_1 + \bar{\alpha}_1 \beta_1) \right],$$

$$g_{02} = -\frac{2\tau'_{10}}{D} \left[\frac{r}{K} + \bar{\beta}_1 \alpha (1 - A_0) + \bar{\alpha}_1^* \phi \bar{\alpha}_1 \bar{\beta}_1 + \bar{\beta}_1^* e \bar{\beta}_1^2 - \bar{\beta}_1^* c_1 \alpha (1 - A_0) \bar{\beta}_1 e^{2i\omega_0\tau'_{10}} - \bar{\beta}_1^* c_2 \phi \bar{\alpha}_1 \bar{\beta}_1 e^{2i\omega_0\tau_2^*} \right],$$

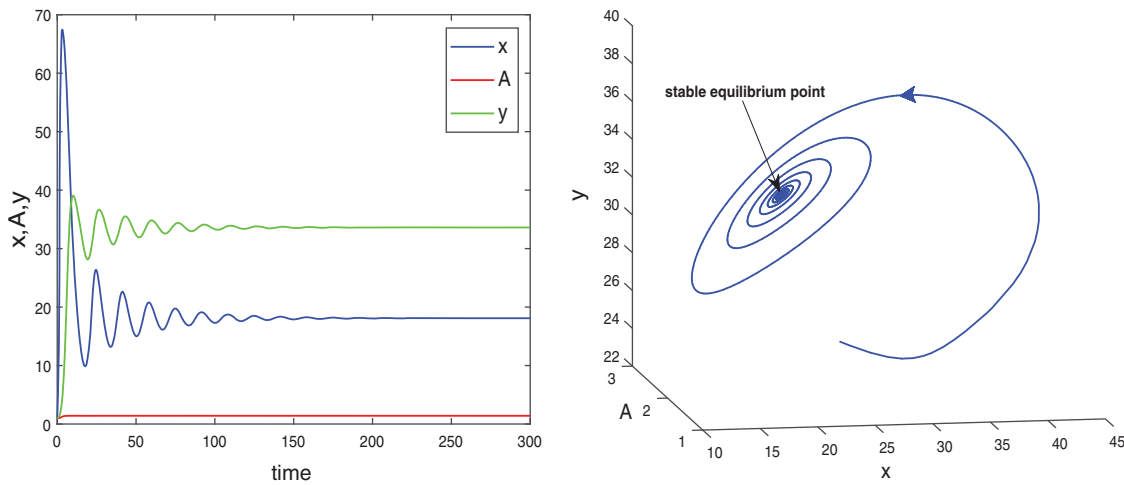


Figure 8: Time series evolution and phase portrait of species for the set of parameters in (25) and $\tau_1 = 0.2 < \tau_{10} = 0.2889$ when $\tau_2 = 0$. System is locally asymptotically stable around the positive equilibrium E^*

$$\begin{aligned}
 g_{21} = & -\frac{2\tau'_{10}}{D} \left[\frac{r}{K} \left\{ 2W_{11}^{(1)}(0) + W_{20}^{(1)}(0) \right\} + \alpha(1 - A_0) \left\{ W_{11}^{(3)}(0) + \frac{1}{2}W_{20}^{(3)}(0) + \frac{1}{2}W_{20}^{(1)}(0) + \beta_1 W_{11}^{(1)}(0) - a\bar{\beta}_1 - 2a\beta_1 \right\} \right. \\
 & + \phi\bar{\alpha}_1^* \left\{ \alpha_1 W_{11}^{(3)}(0) + \frac{1}{2}\bar{\alpha}_1 W_{20}^{(3)}(0) + \frac{1}{2}\bar{\beta}_1 W_{20}^{(2)}(0) + \beta_1 W_{11}^{(2)}(0) \right\} + e\bar{\beta}_1^* \left\{ 2\beta_1 W_{11}^{(3)}(0) + \bar{\beta}_1 W_{20}^{(3)}(0) \right\} \\
 & - \bar{\beta}_1^* c_1 \alpha(1 - A_0) \left\{ e^{-i\omega_0 \tau'_{10}} W_{11}^{(3)}(-1) + \frac{1}{2}e^{i\omega_0 \tau'_{10}} W_{20}^{(3)}(-1) + \frac{1}{2}\bar{\beta}_1 e^{i\omega_0 \tau'_{10}} W_{20}^{(1)}(-1) + \beta_1 e^{-i\omega_0 \tau'_{10}} W_{11}^{(1)}(-1) \right. \\
 & \left. - a\bar{\beta}_1 e^{-i\omega_0 \tau'_{10}} - 2a\beta_1 e^{-i\omega_0 \tau'_{10}} \right\} - c_2 \phi \bar{\beta}_1^* \left\{ \alpha_1 e^{-i\omega_0 \tau_2^*} W_{11}^{(3)}\left(-\frac{\tau_2^*}{\tau'_{10}}\right) + \frac{1}{2}\bar{\alpha}_1 e^{i\omega_0 \tau_2^*} W_{20}^{(3)}\left(-\frac{\tau_2^*}{\tau'_{10}}\right) \right. \\
 & \left. + \frac{1}{2}\bar{\beta}_1 e^{i\omega_0 \tau_2^*} W_{20}^{(2)}\left(-\frac{\tau_2^*}{\tau'_{10}}\right) + \beta_1 e^{-i\omega_0 \tau_2^*} W_{11}^{(2)}\left(-\frac{\tau_2^*}{\tau'_{10}}\right) \right\} \left. \right],
 \end{aligned}$$

where

$$W_{20}(\theta) = \frac{ig_{20}}{\omega_0 \tau'_{10}} q(0) e^{i\omega_0 \tau'_{10} \theta} + \frac{i\bar{g}_{02}}{3\omega_0 \tau'_{10}} \bar{q}(0) e^{-i\omega_0 \tau'_{10} \theta} + E_1 e^{2i\omega_0 \tau'_{10} \theta},$$

$$W_{11}(\theta) = -\frac{ig_{11}}{\omega_0 \tau'_{10}} q(0) e^{i\omega_0 \tau'_{10} \theta} + \frac{i\bar{g}_{11}}{\omega_0 \tau'_{10}} \bar{q}(0) e^{-i\omega_0 \tau'_{10} \theta} + E_2,$$

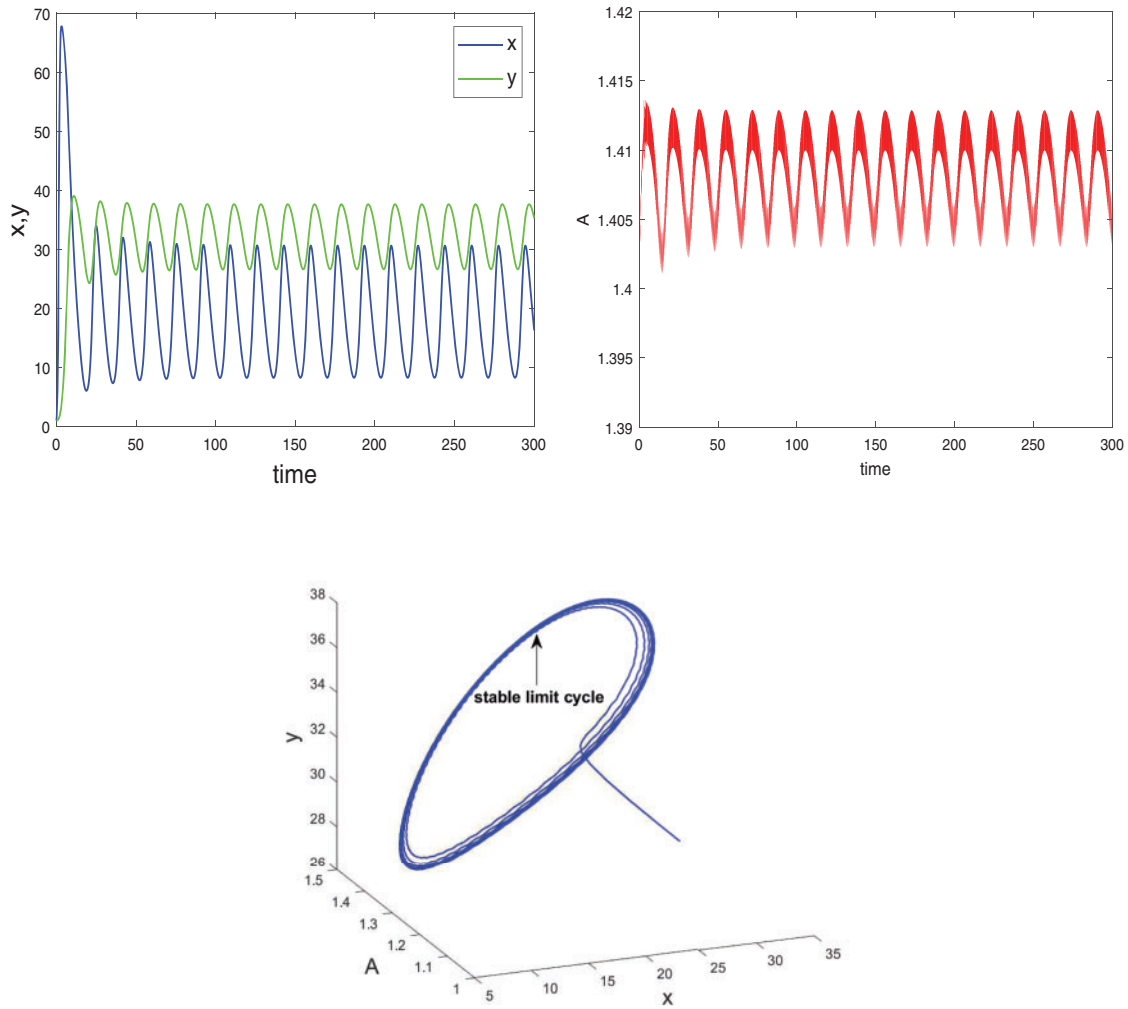


Figure 9: System (2) is unstable when $\tau_1 = 0.35 > \tau_{10} = 0.2889$ and $\tau_2 = 0$. Hopf-bifurcation occurs and stable limit cycle arises in the system

$E_1 = (E_1^{(1)}, E_1^{(2)}, E_1^{(3)})^T \in R^3$ and $E_2 = (E_2^{(1)}, E_2^{(2)}, E_2^{(3)})^T \in R^3$ are constant vectors, computed as:

$$E_1 = 2 \begin{bmatrix} 2i\omega_0 - a_1 & 0 & a_2 \\ 0 & 2i\omega_0 - a_3 & -a_4 \\ -c_1 a_5 e^{-2i\omega_0 \tau'_{10}} & -c_2 \phi y^* e^{-2i\omega_0 \tau_2^*} & 2i\omega_0 - a_6 - c_1 a_2 e^{-2i\omega_0 \tau'_{10}} - c_2 \phi A^* e^{-2i\omega_0 \tau_2^*} \end{bmatrix}^{-1} \\ \times \begin{bmatrix} \frac{r}{K} + \alpha(1 - A_0)\beta_1 \\ \phi\alpha_1\beta_1 \\ e\beta_1^2 - c_1\alpha(1 - A_0)\beta_1 e^{-2i\omega_0 \tau'_{10}} - c_2\phi\alpha_1\beta_1 e^{-2i\omega_0 \tau_2^*} \end{bmatrix},$$

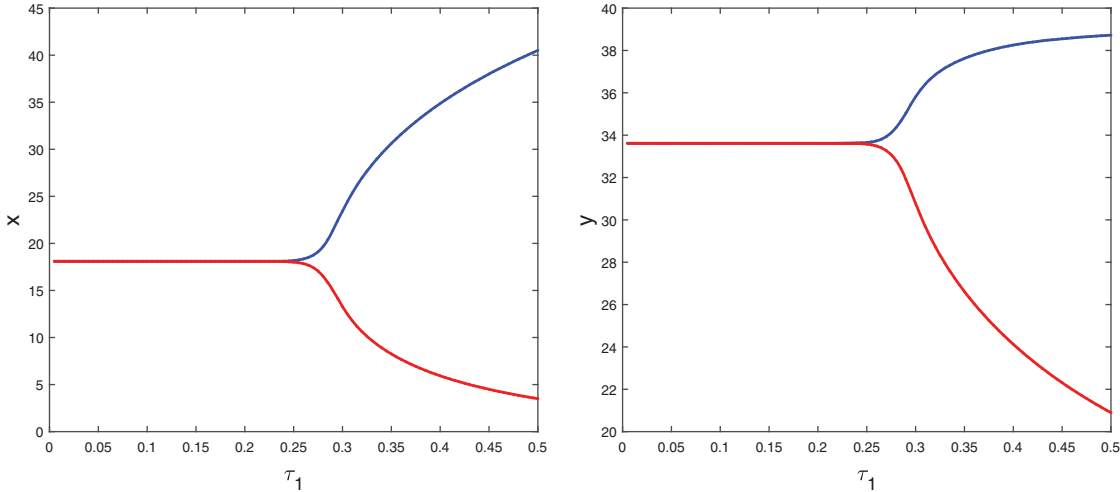


Figure 10: Bifurcation diagram of the prey and predator population with respect to delay parameter τ_1 when $\tau_2 = 0$

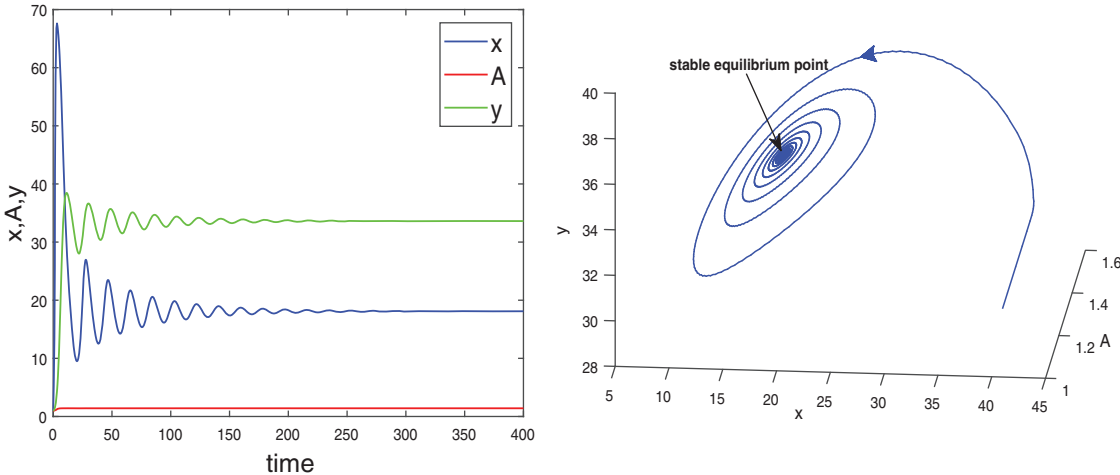


Figure 11: Stable time series solutions and phase diagram of system (2) for $\tau_2 = 0.7 < \tau_{20} = 0.9618$ and $\tau_1 = 0$. Other parameters are same as in (25)

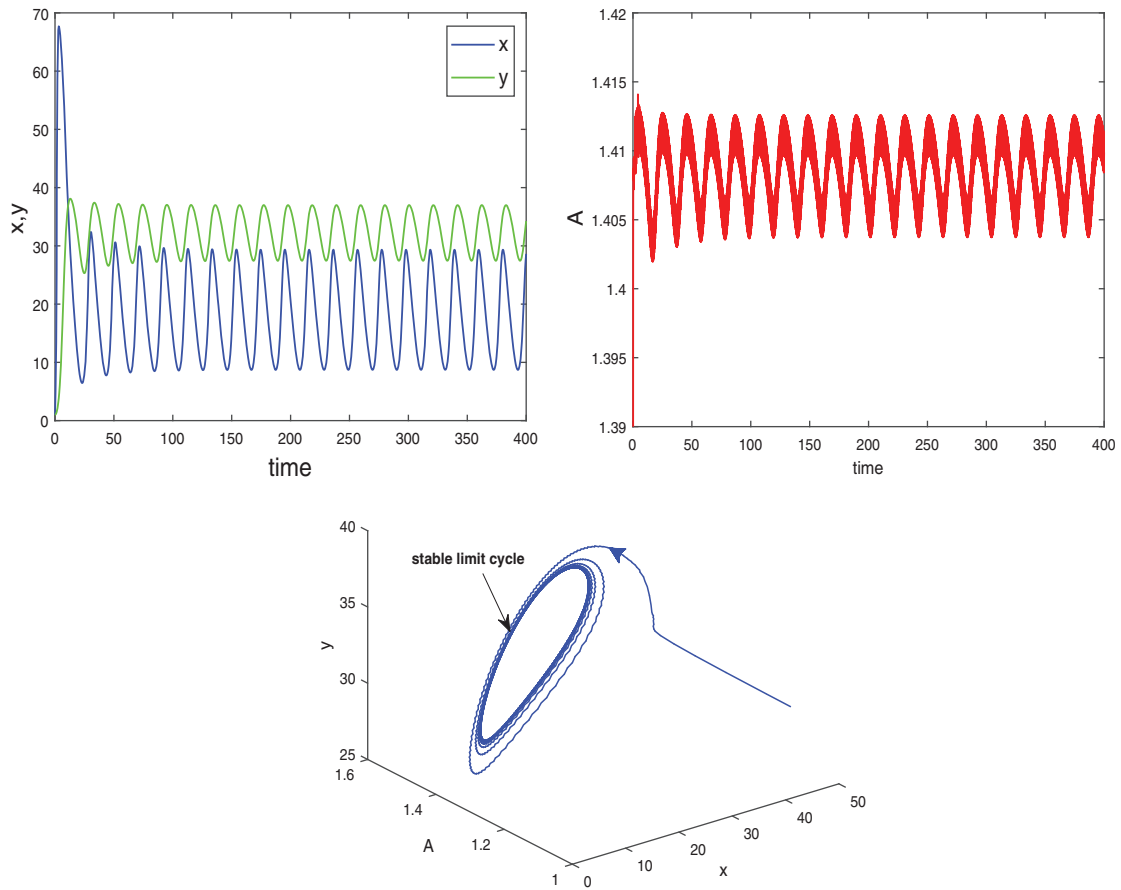


Figure 12: Instable behavior and existence of periodic solutions of system (2) around the positive equilibrium E^* at $\tau_2 = 1.2 > \tau_{2_0} = 0.9618$ and $\tau_1 = 0$

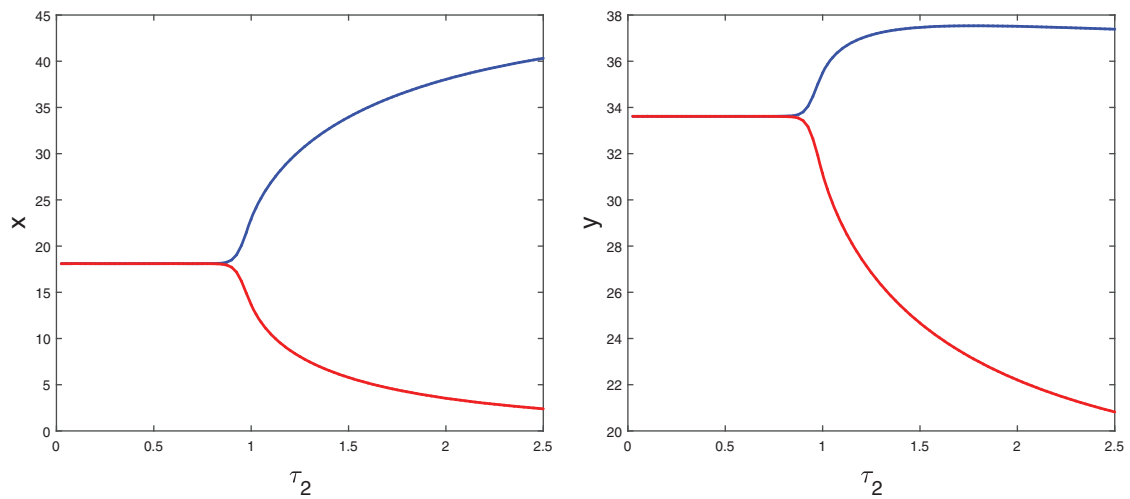


Figure 13: Bifurcation diagram of the prey and predator population with respect to delay parameter τ_2 and $\tau_1 = 0$

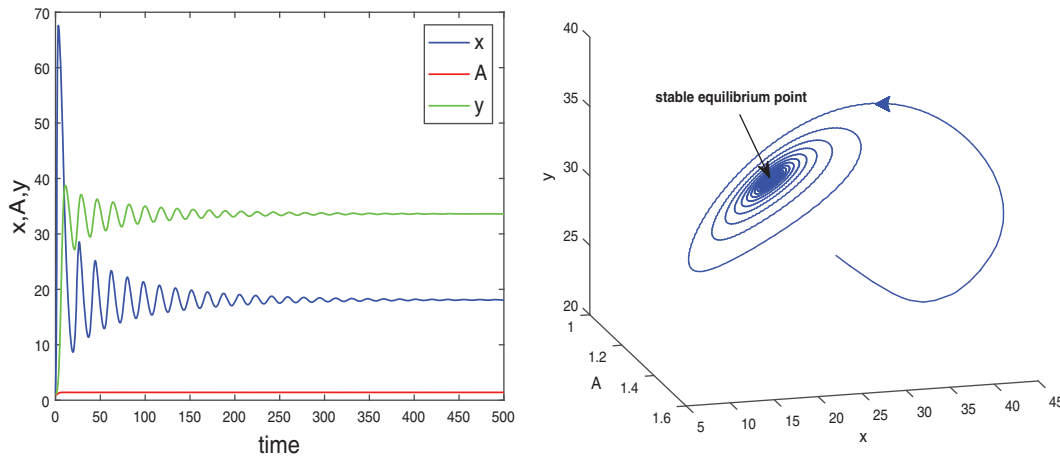


Figure 14: E^* is locally asymptotically stable when $\tau_1 = 0.12$ is fixed in its stable range $(0, \tau_{10})$ and $\tau_2 = 0.4 < \tau'_{20} = 0.4731$

$$E_2 = 2 \begin{bmatrix} -a_1 & 0 & a_2 \\ 0 & -a_3 & -a_4 \\ -c_1 a_5 & -c_2 \phi y^* & -a_6 - c_1 a_2 - c_2 \phi A^* \end{bmatrix}^{-1} \times \begin{bmatrix} \frac{r}{K} + \frac{1}{2} \alpha (1 - A_0) (\beta_1 + \bar{\beta}_1) \\ \frac{1}{2} \phi (\bar{\alpha}_1 \beta_1 + \alpha_1 \bar{\beta}_1) \\ e \beta_1 \bar{\beta}_1 - \frac{1}{2} c_1 \alpha (1 - A_0) (\beta_1 + \bar{\beta}_1) - \frac{1}{2} c_2 \phi (\bar{\alpha}_1 \beta_1 + \alpha_1 \bar{\beta}_1) \end{bmatrix}$$

Consequently, g_{ij} can be expressed by the parameters and delays τ'_{10} and τ_2^* . Thus, these standard results can be computed as:

$$c_1(0) = \frac{i}{2\omega_0 \tau'_{10}} \left(g_{20} g_{11} - 2|g_{11}|^2 - \frac{|g_{02}|^2}{3} \right) + \frac{g_{21}}{2}, \quad \mu_2 = -\frac{Re(c_1(0))}{Re(\lambda'(\tau'_{10}))}$$

$$\beta_2 = 2Re(c_1(0)), \quad T_2 = -\frac{Im(c_1(0)) + \mu_2 Im(\lambda'(\tau'_{10}))}{\omega_0 \tau'_{10}}$$

These expressions give a description of the bifurcating periodic solution in the center manifold of system (2) at critical values $\tau_1 = \tau_{10}$ which can be stated in the form of following theorem:

Theorem 5.1

- μ_2 determines the direction of Hopf-bifurcation. If $\mu_2 > 0 (< 0)$ then the Hopf-bifurcation is supercritical (subcritical).

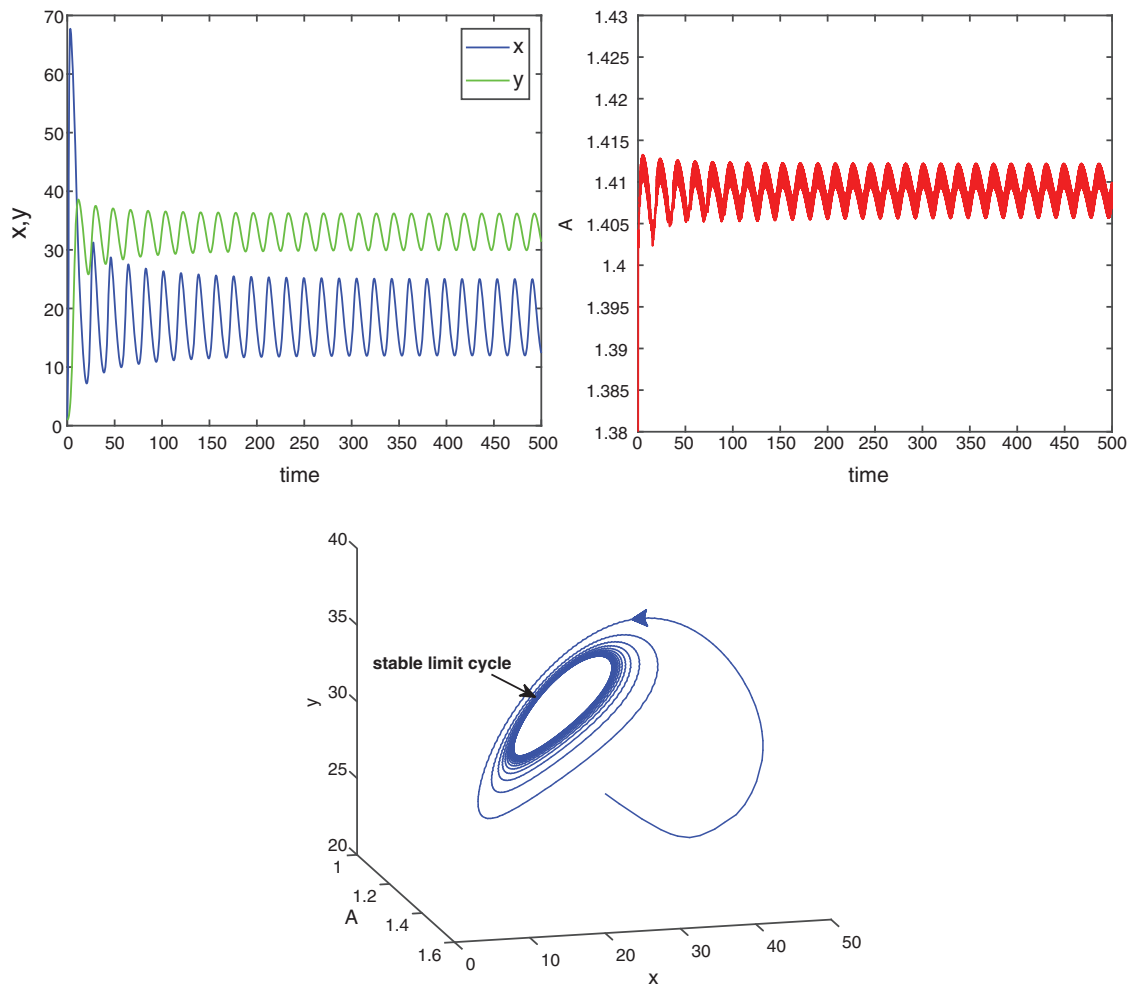


Figure 15: E^* is unstable when $\tau_1 = 0.12$ is fixed in its range of stability $(0, \tau_{1_0})$ and $\tau_2 = 0.6 > \tau'_{2_0} = 0.4731$. Time series solution of species and existence limit cycle

- β_2 determines the stability of bifurcated periodic solution. If $\beta_2 > 0 (< 0)$ then the bifurcated periodic solutions are unstable (stable).
- T_2 determines the period of bifurcating periodic solution. The period increases (decreases) if $T_2 > 0 (< 0)$.

Remark. When $\tau_1 > 0$ and $\tau_2 = 0$ or $\tau_1 = 0$ and $\tau_2 > 0$, then under an analysis similar to Section 5, the corresponding values of μ_2 , β_2 and T_2 can be computed. Depending upon the sign of μ_2 , β_2 and T_2 , the corresponding results can also be deduced.

6 Numerical Simulation of Delayed Model

In order to validate our theoretical findings, obtained in previous sections, we perform some simulations by taking the same values of parameters in (25). We consider all four cases on delay parameters τ_1 and τ_2 .

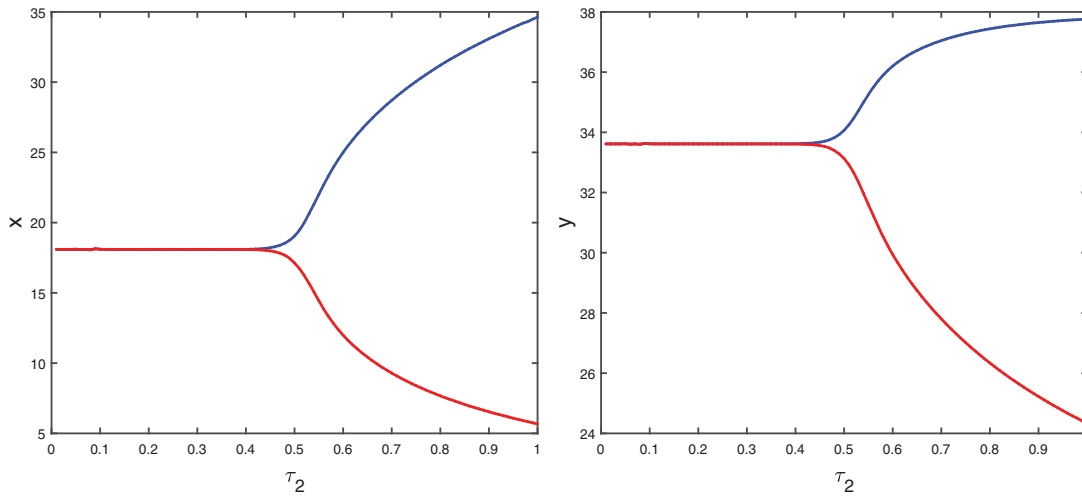


Figure 16: Bifurcation diagram of the prey and predator species with respect to parameter τ_2 when $\tau_1 = 0.12$ is fixed in its range of stability $(0, \tau_{1_0})$

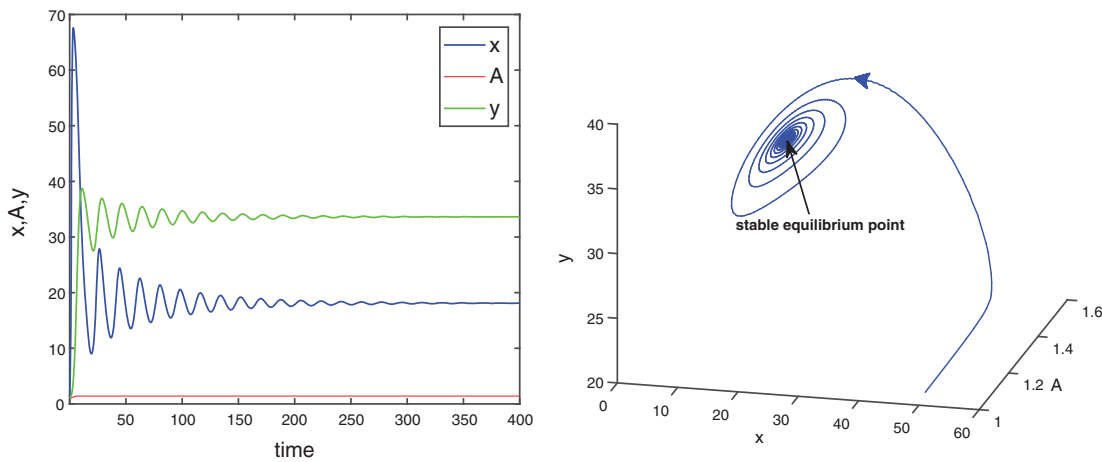


Figure 17: E^* is locally asymptotically stable when $\tau_2 = 0.42$ is fixed in its stable range $(0, \tau'_{2_0})$ and $\tau_1 = 0.1 < \tau_{1_0} = 0.1336$

Case (I): When $\tau_2 = 0$ and $\tau_1 > 0$, then we see that condition (H_1) holds. Since the transversality condition is satisfied, therefore Hopf-bifurcation occurs in the system. To evaluate the critical value of delay parameter, taking $i = 0$ in Eqs. (31) and (32), we obtain

$$\omega_1 = 0.3688, \quad \tau_{1_0} = 0.2889.$$

Thus, the positive equilibrium is locally asymptotically stable for $\tau_1 < \tau_{1_0} = 0.2889$, which is shown in Fig. 8. When $\tau_1 = \tau_{1_0}$, system undergoes a Hopf-bifurcation and periodic solution occurs around E^* . The time series analysis and periodic solution have been shown in Fig. 9. If we starts a trajectory from an initial point then it approaches to the periodic solution (Fig. 9). This shows that the periodic solution is stable. In Fig. 10, we made the bifurcation diagram for both the populations. The blue (red) curve represents the maximum (minimum) values of population at sufficiently large time. It is easy to see that Hopf-bifurcation occurs at $\tau_1 = \tau_{1_0} = 0.2889$.

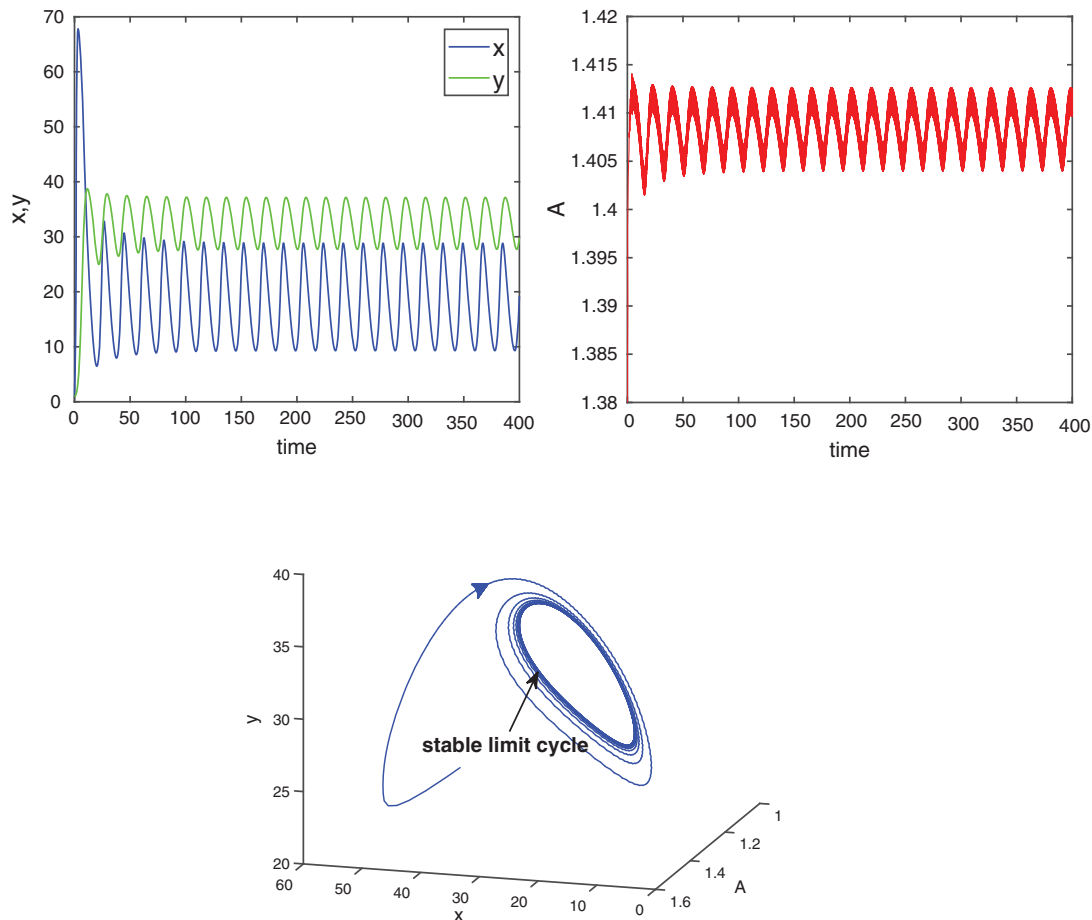


Figure 18: E^* is unstable when $\tau_2 = 0.42$ is fixed in its stable range $(0, \tau_{2_0})$ and $\tau_1 = 0.2 > \tau'_{1_0} = 0.1336$. Time series solution of species and existence limit cycle

Case (II): When $\tau_1 = 0$ and $\tau_2 > 0$. In this case, the transversality condition is satisfied, so the system will show Hopf-bifurcation at a critical value of delay parameter τ_2 . By some computation, we obtain

$$\omega_2 = 0.317, \quad \tau_{2_0} = 0.9618.$$

Therefore, according to our theoretical analysis, the system (2) is locally asymptotically stable for $\tau_2 < \tau_{2_0}$. In Fig. 11, we draw the time series of both the species for $\tau_2 = 0.7 < \tau_{2_0} = 0.9618$. From the figure, it can be seen that system is stable around the positive equilibrium E^* . At $\tau_2 = \tau_{2_0}$, the system goes through a Hopf-bifurcation and for $\tau_2 > \tau_{2_0}$, system becomes unstable and limit cycle produces. This behavior is depicted in Fig. 12. Again bifurcation diagram with respect to delay τ_2 for both the species is drawn in Fig. 13, which helps us to understand the Hopf-bifurcation phenomenon in the system.

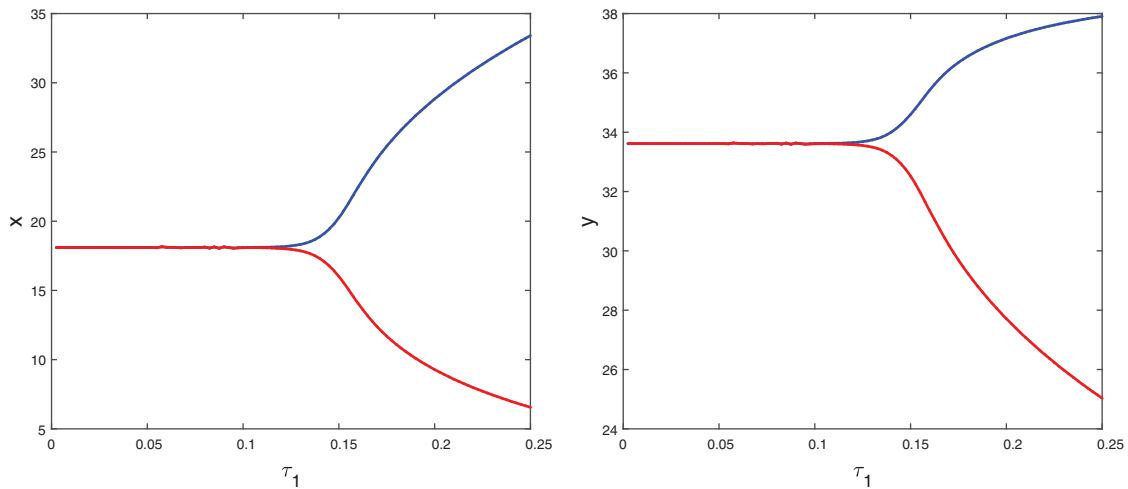


Figure 19: Bifurcation diagram of the prey and predator species with respect to parameter τ_1 when $\tau_2 = 0.42$ is fixed in its stable range $(0, \tau_{2_0})$

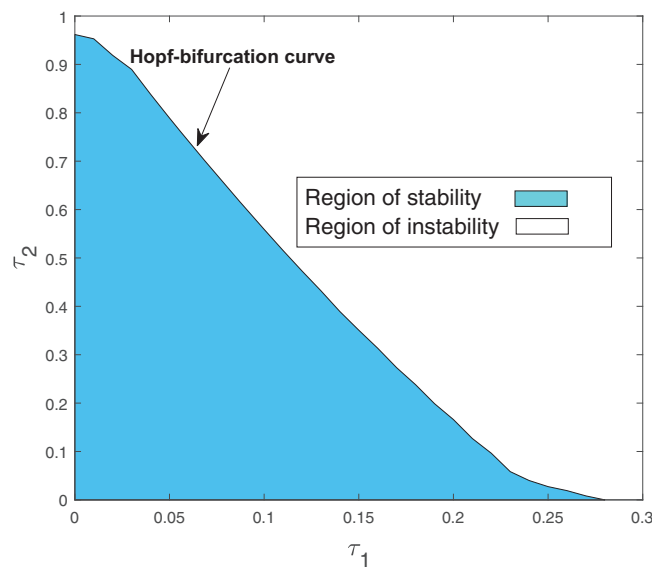


Figure 20: Region of stability and instability for system (2) in $\tau_1\tau_2$ -plane

Case (III): When $\tau_1 = 0.12$ (fixed in the interval $(0, \tau_{1_0})$) and τ_2 as a parameter, then we observe that the condition (H_2) holds true. Therefore according to Theorem 4.4 system (2) undergoes a Hopf-bifurcation. Eqs. (36) and (39) give us the values of ω_0 and τ'_{2_0} as

$$\omega_0 = 0.445, \quad \tau'_{2_0} = 0.4731.$$

Thus the equilibrium point E^* is locally asymptotically stable for $\tau_2 < \tau'_{2_0} = 0.4731$ which is shown in Fig. 14 and unstable for $\tau_2 > \tau'_{2_0}$ (Fig. 15). When $\tau_2 = \tau'_{2_0}$, system undergoes a Hopf-bifurcation around E^* and periodic solution arises in the system. Bifurcation diagram is also presented in Fig. 16 with respect to τ_2 for both the species when $\tau_1 = 0.12$ (fixed).

Case (IV): When $\tau_2 = 0.42$ (fixed in the interval $(0, \tau_{20})$) and τ_1 as a parameter, then our computer simulation yields

$$\omega_* = 0.4491, \quad \tau'_{1_0} = 0.1336.$$

For $\tau_1 = 0.1 \in (0, \tau'_{1_0})$, the system is locally asymptotically stable (Fig. 17). But for $\tau_1 = 0.2 > \tau'_{1_0}$, the system becomes unstable (Fig. 18). Thus the model is stable for $\tau_1 < \tau'_{1_0}$. As τ_1 passes through τ'_{1_0} , it loses the stability and a Hopf-bifurcation occurs in the system. Fig. 18 shows the existence of periodic solution (closed trajectory). The trajectory started from an initial point, approaches to the closed trajectory. This shows that the closed trajectory is stable. In Fig. 19, we present the bifurcation diagram of both the species with respect to τ_1 when $\tau_2 = 0.42$ (fixed).

As the system (2) shows Hopf-bifurcation with respect to both the delay parameters τ_1 and τ_2 . Therefore, we can bisect the $\tau_1\tau_2$ —plane into two regions, which are separated by Hopf-bifurcation curve.

Region of stability (sky blue) $S_3 = \{(\tau_1, \tau_2) : \text{system (2) is locally asymptotically stable}\}$,

Region of instability (white) $S_4 = \{(\tau_1, \tau_2) : \text{system (2) is unstable}\}$.

Both the regions are drawn in Fig. 20.

7 Conclusion

In this study, we have considered a habitat where two biological populations, prey population x and predator population y are surviving and interacting with each other. It is assumed that prey population follows logistic growth in the absence of predator and in the presence of predator, the interaction between them follows Holling type II functional response. We have shown the positivity, boundedness and persistence of the system, which implies that the proposed model is ecologically wellposed. We have defined a parameter A_0 ($0 \leq A_0 \leq 1$) which denotes the dependency of predators on supplied additional food. Our system has four kinds of equilibria, trivial equilibrium $E_0(0, 0, 0)$, axial equilibrium $E_1(K, 0, 0)$, two prey free equilibria \hat{E}_2 and \tilde{E}_2 under condition (5) and unique positive equilibrium E^* under conditions (9) and (10). Local and global stability of the positive equilibrium are shown under several conditions which are dependent upon the parameter A_0 . The parameter A_0 is crucial, so we have studied its effect via Hopf-bifurcation analysis which is also condensed by the numerical illustration. For a chosen set of parameters we calculated the threshold value of parameter A_0 , that is $A_0 = 0.482$, where Hopf-bifurcation occurs and system stabilizes. It is also observed that after stabilization of system if predators are more dependent on additional food then prey population increase whereas predators remain in their range. We also have studied the Hopf-bifurcation with respect to consumption rate of additional food ϕ . Threshold value of ϕ is obtained as $\phi = 0.02847$. In Tab. 3, we have shown the different number of positive equilibrium points by varying the parametric values, when $a = 0.105$ and $d = 0.1$ (other parameters are same as in (25)) then our system has two stable equilibrium together, therefore system shows the phenomenon of bistability, which is depicted in Fig. 7.

Models with delay show comparatively more realistic dynamics than non delayed models. When a predator consumes a prey individual, then its effect does not come immediately, it takes some time i.e., time lag for gestation. Again, predators also take some time to consume and digest the supplied additional food to them. Therefore, to make our model ecologically more realistic,

we incorporated two delays; one for gestation delay and other for consuming and digesting the supplied additional food.

For the delayed model, we have analyzed Hopf-bifurcation via local stability taking delay as a bifurcation parameter. We investigated the Hopf-bifurcation phenomenon for all combinations of both delays. We obtained the sufficient conditions for the stability of the positive equilibrium point and existence of Hopf-bifurcation for Case(1): $\tau_1 > 0$, $\tau_2 = 0$, Case(2): $\tau_1 = 0$, $\tau_2 > 0$, Case(3): τ_1 is fixed in the interval $(0, \tau_{1_0})$ and τ_2 as a variable parameter, Case(4): τ_2 is fixed in the interval $(0, \tau_{2_0})$ and τ_1 as a variable parameter. Our system undergoes Hopf-bifurcation in the vicinity of the interior equilibrium point with respect to both the delay parameters when they cross their critical values. The qualitative properties of Hopf-bifurcation are studied by using the Normal form theory and the formulae given in Hassard et al. [34].

We have performed some numerical simulations to illustrate our theoretical results. For a biologically feasible set of parameters, the system is stable initially, then we introduce delay and system remains stable till its critical value. If we increase the delay parameter over the critical value, then system goes through Hopf-bifurcation and becomes unstable. Bifurcation diagrams (Figs. 10, 13, 16, 19) with respect to different delays depict the dynamical behavior of the system.

Our study is important to conserve the prey population through providing additional food to predators and to establish their balance. Here we have also shown the significance of delay parameters. We hope that this study will help to perceive the dynamics of an ecological system with additional food and two discrete delays.

Acknowledgement: The author (Ankit Kumar) acknowledges the Junior Research Fellowship received from University Grant Commission, New Delhi, India.

Funding Statement: The authors received no specific funding for this study.

Conflicts of Interest: The authors declare that they have no conflicts of interest to report regarding the present study.

References

1. Lotka, A. J. (1925). *Elements of physical biology*. Baltimore, New York: Williams and Wilkins.
2. Volterra, V. (1927). *Variazioni e fluttuazioni del numero d'individui in specie animali conviventi*. Venezia, C. Ferrari.
3. Ma, Z., Wang, S. (2018). A delay-induced predator-prey model with Holling type functional response and habitat complexity. *Nonlinear Dynamics*, 93(3), 1519–1544. DOI 10.1007/s11071-018-4274-2.
4. Dubey, B., Kumar, A., Maiti, A. P. (2019). Global stability and Hopf-bifurcation of prey–predator system with two discrete delays including habitat complexity and prey refuge. *Communications in Nonlinear Science and Numerical Simulation*, 67, 528–554. DOI 10.1016/j.cnsns.2018.07.019.
5. Holling, C. S. (1959). The components of predation as revealed by a study of small-mammal predation of the European pine sawfly. *The Canadian Entomologist*, 91(5), 293–320. DOI 10.4039/Ent91293-5.
6. Crowley, P. H., Martin, E. K. (1989). Functional responses and interference within and between year classes of a dragonfly population. *Journal of the North American Benthological Society*, 8(3), 211–221. DOI 10.2307/1467324.
7. Wang, W., Chen, L. (1997). A predator–prey system with stage–structure for predator. *Computers & Mathematics with Applications*, 33(8), 83–91. DOI 10.1016/S0898-1221(97)00056-4.
8. Faria, T. (2001). Stability and bifurcation for a delayed predator–prey model and the effect of diffusion. *Journal of Mathematical Analysis and Applications*, 254(2), 433–463. DOI 10.1006/jmaa.2000.7182.

9. Prasad, B. S. R. V., Banerjee, M., Srinivasu, P. D. N. (2013). Dynamics of additional food provided predator–prey system with mutually interfering predators. *Mathematical Biosciences*, 246(1), 176–190. DOI 10.1016/j.mbs.2013.08.013.
10. Li, H., Meng, G., She, Z. (2016). Stability and Hopf bifurcation of a delayed density–dependent predator–prey system with Beddington–DeAngelis functional response. *International Journal of Bifurcation and Chaos*, 26(10), 1650165. DOI 10.1142/S0218127416501650.
11. Wang, X., Zanette, L., Zou, X. (2016). Modelling the fear effect in predator–prey interactions. *Journal of Mathematical Biology*, 73(5), 1179–1204. DOI 10.1007/s00285-016-0989-1.
12. Li, H. L., Zhang, L., Hu, C., Jiang, Y. L., Teng, Z. (2017). Dynamical analysis of a fractional-order predator–prey model incorporating a prey refuge. *Journal of Applied Mathematics and Computing*, 54(1–2), 435–449. DOI 10.1007/s12190-016-1017-8.
13. Dong, Q., Ma, W., Sun, M. (2013). The asymptotic behavior of a chemostat model with Crowley–Martin type functional response and time delays. *Journal of Mathematical Chemistry*, 51(5), 1231–1248. DOI 10.1007/s10910-012-0138-z.
14. Maiti, A. P., Dubey, B., Tushar, J. (2017). A delayed prey–predator model with Crowley–Martin-type functional response including prey refuge. *Mathematical Methods in the Applied Sciences*, 40(16), 5792–5809. DOI 10.1002/mma.4429.
15. Srinivasu, P. D. N., Prasad, B. S. R. V., Venkatesulu, M. (2007). Biological control through provision of additional food to predators: A theoretical study. *Theoretical Population Biology*, 72(1), 111–120.
16. Ddumba, H., Mugisha, J. Y. T., Gonsalves, J. W., Kerley, G. I. H. (2013). Periodicity and limit cycle perturbation analysis of a predator–prey model with interspecific species’ interference, predator additional food and dispersal. *Applied Mathematics and Computation*, 219(15), 8338–8357. DOI 10.1016/j.amc.2012.11.063.
17. Sahoo, P., Poria, S. (2014). The chaos and control of a food chain model supplying additional food to top-predator. *Chaos, Solitons & Fractals*, 58, 52–64.
18. Kumar, D., Chakrabarty, S. P. (2015). A comparative study of bioeconomic ratio-dependent predator–prey model with and without additional food to predators. *Nonlinear Dynamics*, 80(1–2), 23–38.
19. Sen, M., Srinivasu, P. D. N., Banerjee, M. (2015). Global dynamics of an additional food provided predator–prey system with constant harvest in predators. *Applied Mathematics and Computation*, 250, 193–211.
20. Ghosh, J., Sahoo, B., Poris, S. (2017). Prey-predator dynamics with prey refuge providing additional food to predator. *Chaos, Solitons & Fractals*, 96, 110–119.
21. Sahoo, B. (2015). Role of additional food in eco-epidemiological system with disease in the prey. *Applied Mathematics and Computation*, 259, 61–79. DOI 10.1016/j.amc.2015.02.038.
22. Rani, R., Gakkhar, S. (2019). The impact of provision of additional food to predator in predator–prey model with combined harvesting in the presence of toxicity. *Journal of Applied Mathematics and Computing*, 60(1–2), 673–701. DOI 10.1007/s12190-018-01232-z.
23. Bairagi, N., Jana, D. (2011). On the stability and Hopf bifurcation of a delay-induced predator–prey system with habitat complexity. *Applied Mathematical Modelling*, 35(7), 3255–3267. DOI 10.1016/j.apm.2011.01.025.
24. Tripathi, J. P., Abbas, S., Thakur, M. (2015). A density dependent delayed predator–prey model with Beddington–DeAngelis type function response incorporating a prey refuge. *Communications in Nonlinear Science and Numerical Simulation*, 22(1–3), 427–450. DOI 10.1016/j.cnsns.2014.08.018.
25. Gourley, S. A., Kuang, Y. (2004). A stage structured predator–prey model and its dependence on maturation delay and death rate. *Journal of Mathematical Biology*, 49(2), 188–200. DOI 10.1007/s00285-004-0278-2.
26. Song, Y., Wei, J. (2004). Bifurcation analysis for Chen’s system with delayed feedback and its application to control of chaos. *Chaos, Solitons & Fractals*, 22(1), 75–91. DOI 10.1016/j.chaos.2003.12.075.
27. Qu, Y., Wei, J. (2007). Bifurcation analysis in a time-delay model for prey–predator growth with stage-structure. *Nonlinear Dynamics*, 49(1–2), 285–294. DOI 10.1007/s11071-006-9133-x.
28. Misra, A. K., Dubey, B. (2010). A ratio-dependent predator–prey model with delay and harvesting. *Journal of Biological Systems*, 18(2), 437–453. DOI 10.1142/S021833901000341X.

29. Chakraborty, K., Jana, S., Kar, T. K. (2012). Effort dynamics of a delay-induced prey–predator system with reserve. *Nonlinear Dynamics*, 70(3), 1805–1829.
30. Gakkhar, S., Singh, A. (2012). Complex dynamics in a prey predator system with multiple delays. *Communications in Nonlinear Science and Numerical Simulation*, 17(2), 914–929. DOI 10.1016/j.cnsns.2011.05.047.
31. Jana, S., Chakraborty, M., Chakraborty, K., Kar, T. K. (2012). Global stability and bifurcation of time delayed prey–predator system incorporating prey refuge. *Mathematics and Computers in Simulation*, 85, 57–77. DOI 10.1016/j.matcom.2012.10.003.
32. Misra, A. K., Lata, K. (2013). Modeling the effect of time delay on the conservation of forestry biomass. *Chaos, Solitons & Fractals*, 46, 1–11. DOI 10.1016/j.chaos.2012.10.002.
33. Liu, Y., Zhang, X., Zhou, T. (2014). Multiple periodic solutions of a delayed predator–prey model with non-monotonic functional response and stage structure. *Journal of Biological Dynamics*, 8(1), 145–160.
34. Hassard, B. D., Kazarinoff, N. D., Wan, Y. H., Wan, Y. W. (1981), *Theory and applications of Hopf bifurcation*. vol. 41. London, UK: CUP Archive.
35. Sahoo, B., Poria, S. (2015). Effects of additional food in a delayed predator–prey model. *Mathematical Biosciences*, 261, 62–73. DOI 10.1016/j.mbs.2014.12.002.
36. Mondal, S., Maiti, A., Samanta, G. P. (2019). Effects of fear and additional food in a delayed predator–prey model. *Biophysical Reviews and Letters*, 13(4), 157–177. DOI 10.1142/S1793048018500091.
37. Li, K., Wei, J. (2009). Stability and Hopf bifurcation analysis of a prey–predator system with two delays. *Chaos, Solitons & Fractals*, 42(5), 2606–2613. DOI 10.1016/j.chaos.2009.04.001.
38. Xu, C., Tang, X., Liao, M., He, X. (2011). Bifurcation analysis in a delayed Lotka–Volterra predator–prey model with two delays. *Nonlinear Dynamics*, 66(1–2), 169–183. DOI 10.1007/s11071-010-9919-8.
39. Xu, C., Li, P. (2012). Dynamical analysis in a delayed predator–prey model with two delays. *Discrete Dynamics in Nature and Society*, 2012(1), 1–22. DOI 10.1155/2012/652947.
40. Kundu, S., Maitra, S. (2018). Dynamical behaviour of a delayed three species predator–prey model with cooperation among the prey species. *Nonlinear Dynamics*, 92(2), 627–643. DOI 10.1007/s11071-018-4079-3.
41. Misra, A. K., Verma, M. (2013). A mathematical model to study the dynamics of carbon dioxide gas in the atmosphere. *Applied Mathematics and Computation*, 219(16), 8595–8609. DOI 10.1016/j.amc.2013.02.058.
42. Carr, J. (2012). *Applications of centre manifold theory*, vol. 35. Berlin, Germany: Springer Science & Business Media.
43. Kuznetsov, Y. A. (2013), *Elements of applied bifurcation theory*. vol. 112. Berlin, Germany: Springer Science & Business Media.
44. Lin, Y., Zeng, X., Jing, Z. (1996). Dynamical behaviors for a three-dimensional differential equation in chemical system. *Acta Mathematicae Applicatae Sinica*, 12(2), 144–154. DOI 10.1007/BF02007734.